Acknowledgment. This work has been supported by the Deutsche Forschungsgemeinschaft, Bonn, Fonds der Chemischen Industrie, Frankfurt; and the DEGUSSA AG, Hanau, Germany, which are gratefully acknowledged.

Registry No. **3a**, 98088-31-4; **3b**, 98088-32-5; **4a**, 112713-06-1; **4b**, 112713-07-2; **5a**, 112713-09-4; **5b**, 112713-08-3; $Me_2S(O{=}CH_2$, 70775-39-2; $[C\text{-}C_3H_5SPh_2)BF_4$, 33462-81-6.

Supplementary Material Available: Tables of crystal data, atom coordinates and isotropic thermal parameters, bond distances, bond angles, anisotropic thermal parameters, and hydrogen atom coordinates and isotropic thermal parameters (9 pages); a listing of observed and calculated structure factors (44 pages). Ordering information is given on any current masthead page.

Cationic Complexes of Rhodium(I) and Iridium(I) with Methyl- and Phenylbis(dimethoxyphosphino)amine

Joel T. Mague* and Charles L. Lloyd

Department of Chemistry, Tulane University, New Orleans, Louisiana 70118

Received September 21, 1987

The ligand $PhN(P(OMe)_2)_2$ (L_2) reacts with $[Rh(COD)(acetone)_x]ClO_4$ to form $[Rh(COD)(L_2)]ClO_4$, $[Rh(L_2)_2]ClO_4$, and $[Rh_2(L_2)_4(\mu\text{-}L_2)](ClO_4)_2$ depending on the metal/ligand ratio used. By contrast $MeN(P(OMe)_2)_2$ (L_2') only forms $[Rh_2(L_2')_2(\mu\text{-}L_2')_2]^{2+}$ which was isolated as PF_6^-, BPh_4^-, ClO_4^-, and $F_3CSO_3^-$ salts. Other rhodium complexes of the latter ligand that were synthesized include $[Rh(L_2')(DPPE)]ClO_4$, $[Rh(L)(L_2')(DPPE)]ClO_4$ (L = CO, $P(OMe)_3$), and $[Rh_2(L_2')_2(\mu\text{-}L_2'')_2](ClO_4)_2$ (L_2'' = 2,5-bis(diphenylphosphino)furan). The iridium analogue of the latter was also prepared as were several iridium complexes of $MeN(P(OMe)_2)_2$ including $[Ir(L_2')(PPh_3)_2]ClO_4$, $[Ir(L_2')_2(PPh_3)]ClO_4$, $[Ir(CO)(L_2')(PPh_3)_2]ClO_4$, $[Ir(L_2')_3]ClO_4$, and $[Ir(L_2')(BDPPF)]ClO_4$. The last appears to form five-coordinate adducts with O_2 and dimethyl acetylenedicarboxylate. With the exception of these last two, all the five-coordinate complexes prepared are proposed to adopt fluxional trigonal-bipyramidal structures. $[Ir(CO)(L_2')(PPh_3)_2]ClO_4$ crystallizes in the monoclinic system with space group $P2_1/c$, $a = 16.067$ (2) Å^2, $b = 14.421$ (2) Å, $c = 1.9574$ (4) Å, $\beta = 102.49$ (1)°, and $Z = 4$. Full-matrix least-squares refinement of 341 variables using 5462 data ($I > 3\sigma(I)$) led to final values of R and R_w of 0.037 and 0.048, respectively. The perchlorate ion is partially disordered. The complex adopts a distorted trigonal-bipyramidal structure with an equatorial carbonyl ligand. $[Rh_2(L_2')_4](F_3CSO_3)_2$ crystallizes in the monoclinic system with space group $P2_1/c$, $a = 22.676$ (4) Å, $b = 19.079$ (4) Å, $c = 12.236$ (7) Å, $\beta = 97.12$ (3)°, and $Z = 4$. Full-matrix least-squares refinement of 523 variables using 6097 data ($I > 3\sigma(I)$) led to final values of R and R_w of 0.055 and 0.083, respectively. One anion is severely disordered. The dimer cation contains two distorted square-planar rhodium atoms bridged by two $MeN(P(OMe)_2)_2$ ligands situated cis to one another. The coordination sphere of each metal is completed by a second ligand which chelates resulting in a basket-shaped species.

Introduction

We have been engaged for several years in studies on the synthesis of binuclear complexes of the short-bite ligands bis(diphenylphosphino)methane (DPM) and its arsenic analogue (DAM) and their reactivity toward small organic and inorganic molecules.[1] From this work and related studies by others[2] it has become increasingly evident that the bulk of the phenyl groups on these ligands significantly restricts access to the metal atoms. In considering sterically less-demanding ligands with which it was hoped to prepare related binuclear complexes that would have the potential to bind a larger variety of substrates we chose $MeN(P(OMe)_2)_2$.[3] This was attractive because of its relative ease of synthesis and handling and because it had already been found to form a binuclear complex of cobalt[3] while $EtN(P(OMe)_2)_2$ also formed suitable binuclear rhodium complexes.[4] Apart from this brief report and others on rhodium complexes of $EtN(P(OPh)_2)_2$[5] and iridium complexes of $RN(PPh_2)_2$ (R = H, Me, Ph, β-tolyl)[6] the ligating properties of this class of ligands toward platinum group metals has not been investigated. We report here on the results of our efforts to expand this area which, unfortunately, did not yield any of the desired binuclear complexes.

Experimental Section

All solvents were appropriately dried and distilled prior to use and were stored under dinitrogen. All operations were performed under a dinitrogen atmosphere although most of the products proved not be to particularly sensitive to the ambient atmosphere. Standard Schlenk techniques were used. Hydrated rhodium(III) chloride, silver perchlorate, and silver trifluoromethanesulfonate

---

(1) (a) Mague, J. T.; DeVries, S. H. *Inorg. Chem.* **1982**, *21*, 1632. (b) Mague, J. T. *Inorg. Chem.* **1983**, *22*, 45. (c) Mague, J. T. *Inorg. Chem.* **1983**, 22, 1158. (d) Mague, J. T.; Klein, C. L.; Majeste, R. J.; Stevens, E. D. *Organometallics* **1984**, *3*, 1860. (e) Mague, J. T. *Organometallics* **1986**, *5*, 918.

(2) (a) Sutherland, B. R.; Cowie, M. *Can. J. Chem.* **1986**, *64*, 464. (b) Kubiak, C. P.; Eisenberg, R. *Inorg. Chem.* **1980**, *19*, 2726. (c) Kubiak, C. P.; Woodcock, C.; Eisenberg, R. *Inorg. Chem.* **1980**, *19*, 2733.

(3) Brown, G. M.; Finholt, J. E.; King, R. B.; Bibber, J. W. *Inorg. Chem.* **1982**, *21*, 2139.

(4) Haines, R. J.; Laing, M.; Meintjies, W.; Sommerville, P. *J. Organomet. Chem.* **1981**, *215*, C17.

(5) (a) Haines, R. J.; Meintjies, E.; Laing, M.; Sommerville, P. *J. Organomet. Chem.* **1981**, *216*, C19. (b) Field, J. S.; Haines, R. J.; Meintjies, E.; Sigwarth, B.; Van Rooyen, P. H. *J. Organomet. Chem.* **1984**, *268*, C43. (c) Haines, R. J.; Meintjies, E.; Laing, M. *Inorg. Chim. Acta* **1979**, *36*, L403.

(6) (a) Ellermann, J.; Mader, L. *Z. Naturforsch., B: Anorg. Chem., Org. Chem.* **1980**, *35b*, 307. (b) Ellermann, J.; Giebel, K.; Mader, L.; Moll, M. *Chem. Ber.* **1981**, *114*, 2322. (c) Ellermann, J.; Mader, L.; Giebel, K. *Z. Naturforsch., B: Anorg. Chem., Org. Chem.* **1981**, *36B*, 571.

0276-7333/88/2307-0983$01.50/0

(triflate) were purchased from Alfa Inorganics while ammonium hexachloroiridate(IV) was obtained from available laboratory residues of iridium using the published procedure.[7] Literature procedures were also used to prepare $MeN(P(OMe)_2)_2$,[3] $PhN(PCl_2)_2$,[8] $[(\eta^5\text{-}C_5H_4PPh_2)_2Fe]$(BDPPF),[9] 2,5-bis(diphenylphosphino)furan,[10] $[IrCl(COD)]_2$ (COD = cycloocta-1,5-diene),[11] $[Ir(COD)(PPh_3)_2]ClO_4$,[12] and $[Rh(COD)(DPPE)]ClO_4$ (DPPE = 1,2-bis(diphenylphosphino)ethane).[12] $[RhCl(COD)]_2$ was prepared by an adaptation of the method used for $[IrCl(COD)]_2$ which gives superior yields to the literature method.[13] Carbon monoxide was CP grade, and all other reagents were of laboratory grade and were used without further purification unless otherwise noted. Infrared spectra were obtained on a Perkin-Elmer 683 spectrometer or a Matson Cygnus 100 FTIR spectrometer as Nujol mulls unless otherwise specified. Proton and noise-decoupled phosphorus-31 NMR spectra were obtained on an IBM/Bruker AF-200 spectrometer at 200.13 and 81.02 MHz, respectively, using a 45° pulse and repetition times of 2.9 and 4.5 s, respectively. Proton and phosphorus chemical shifts are referred to external tetramethylsilane (δ 0.0) and external 85% H_3PO_4 (δ 0.0), respectively, using the high-frequency positive convention. All spectra were obtained at ambient probe temperature (ca. 30 °C) unless otherwise specified. Spectral simulations were performed with the PANIC program supplied as part of the software of the AF-200 spectrometer system. Analyses were performed by Galbraith Laboratories, Inc., Knoxville, TN.

Synthesis of $C_6H_5N(P(OCH_3)_2)_2$. This was prepared by using the same procedure reported for $MeN(P(OMe)_2)_2$[3] from $PhN(PCl_2)_2$ which had been crystallized from phosphorus trichloride. Following removal of the triethylammonium chloride by filtration and most of the diethyl ether by distillation, the residue was placed under a dynamic vacuum at room temperature for several hours until no volatile material remained. The cloudy, pale yellow oil that remained was vacuum distilled by using a short-path apparatus to provide ca. 10 mL of a colorless, viscous liquid (bp 92 °C (0.03 mm)): ^1H NMR ($(CD_3)_2CO$) δ 7.0–7.4 (m, 5 H, C_6H_5),[14] 3.48 (apparent triplet, J = 6.4 Hz, 12 H, OCH_3); $^{31}P\{^1H\}$ NMR ($(CD_3)_2CO$) δ 142.5 (s). The ligand appears subject to thermal decomposition since at the point the distillation was terminated, at least 10 mL of material remained in the pot and had become quite dark in color. Also, in a prior attempt at purification using a normal fractionation setup, little if any of the desired compound was obtained and much dark colored material remained in the pot.

Caution. Perchlorate salts are notoriously unpredictable with respect to shock and thermal instability. No problems were encountered with those synthesized here, but due care should always be exercised when working with them.

$[Rh(c\text{-}C_8H_{12})(C_6H_5N(P(OCH_3)_2)_2)]ClO_4$ (1). A mixture of $[RhCl(COD)]_2$ (0.200 g, 0.405 mmol) and silver perchlorate (0.168 g, 0.810 mmol) in 20 mL of acetone was stirred for 0.5 h and filtered through a pad of diatomaceous earth to remove precipitated silver chloride. Addition of 0.225 g (0.810 mmol) of a toluene solution of $PhN(P(OMe)_2)_2$ to the yellow filtrate caused it to become a dark magenta, but on stirring the color soon changed to a clear orange. Concentration under reduced pressure and dilution with hexane afforded the product as orange crystals in 70% yield: ^1H NMR ($(CD_3)_2CO$) δ 7.2–7.5 (m, 5 H, C_6H_5), 6.05 (s, 4 H, COD), 4.08 (m, 12 H, OCH_3), 2.4–2.8 (m, 8 H, COD); $^{31}P\{^1H\}$ NMR ($(CD_3)_2CO$) δ 103.7 (d, $^1J_{Rh-P}$ = 225.2 Hz). Anal. Calcd for $C_{18}H_{29}P_2O_8NClRh$: C, 36.79; H, 4.949 Found: C, 36.8; H, 4.8.

$[Rh(C_6H_5N(P(OCH_3)_2)_2)_2]ClO_4$ (2). This was prepared in an analogous fashion to that used for 1 but with twice the quantity of ligand. It was obtained in 20% yield following dilution with diethyl ether and recrystallization from acetone/hexane. The major product is an orange oil that has so far defied characterization: ^1H NMR ($(CD_3)_2CO$) δ 7.3–7.7 (m, 5 H, C_6H_5), 4.04 (br, 12 H, OCH_3); $^{31}P\{^1H\}$ NMR ($(CD_3)_2CO$) δ 121.2 (d, $^1J_{Rh-P}$ = 182.3 Hz). Anal. Calcd for $C_{20}H_{34}P_4O_{12}N_2ClRh$: C, 31.76; H, 4.49. Found: C, 32.3; H, 4.5.

$[Rh_2(C_6H_5N(P(OCH_3)_2)_2)_5](ClO_4)_2\cdot 2(CH_3)_2CO$ (3). This was prepared in a manner analogous to 1 but with a ligand/metal ratio of 3 and obtained in 60% yield as yellow crystals following dilution with diethyl ether. The presence of the solvent acetone was confirmed by the ^1H NMR spectrum: ^1H NMR (CD_2Cl_2) δ 6.9–7.5 (m, 25 H, C_6H_5), 3.71–3.81 (m, 48 H, OCH_3), 3.68 (d, $^3J_{P-H}$ = 9.9 Hz, 12 H, OCH_3), 2.12 (s, acetone); $^{31}P\{^1H\}$ NMR (CD_2Cl_2) δ(P) 146.2 (dquin), δ(P′) 109.5 (dd) ($^2J_{P-P'}$ = 55.1, $^1J_{Rh-P}$ = 196.1, $^1J_{Rh-P'}$ = 157.6 Hz). Anal. Calcd for $C_{56}H_{97}O_{30}P_{10}N_5Cl_2Rh_2$: C, 35.27; H, 5.14. Found: C, 35.2; H, 4.8.

$[Rh(H_3CN(P(OCH_3)_2)_2)((C_6H_5)_2PCH_2CH_2P(C_6H_5)_2)]ClO_4$ (4). A toluene solution of $MeN(P(OMe)_2)_2$ (0.087 g, 0.400 mmol) was added dropwise to a solution of $[Rh(COD)(DPPE)]ClO_4$ (0.250 g, 0.350 mmol) in 15 mL of dichloromethane whereupon the solution became bright yellow. After being stirred for 5 h, the solution was concentrated under reduced pressure and diluted with diethyl ether. Recrystallization of the crude product from acetone/diethyl ether afforded yellow crystals in 75% yield: ^1H NMR ($(CD_3)_2CO$) δ 7.4–7.8 (m, 20 H, C_6H_5), 3.55 (m, 12 H, OCH_3), 2.56 (t, $^3J_{P_A-H}$ = 10.4 Hz, 3 H, NCH_3), 2.4–2.6 (m, 4 H, CH_2CH_2); $^{31}P\{^1H\}$ NMR ($(CD_3)_2CO$) $\delta(P_A)$ 115.8, $\delta(P_B)$ 59.1 (AA′BB′X (X = Rh) ($J_{P_A-P_{A'}}$ = −30.1, $J_{P_B-P_{B'}}$ = 63.7, $J_{P_A-P_B} = J_{P_{A'}-P_{B'}}$ = 378.7, $J_{P_A-P_{B'}} = J_{P_{A'}-P_B}$ = −36.3, $^1J_{P_A-Rh} = {}^1J_{P_{A'}-Rh}$ = 188.4, $^1J_{P_B-Rh} = {}^1J_{P_{B'}-Rh}$ = 126.6 Hz). Anal. Calcd for $C_{31}H_{39}P_4O_8NClRh$: C, 45.65; H, 4.78; N, 1.72. Found: C, 45.8; H, 4.8; N, 1.5.

$[Rh(P(OCH_3)_3)(H_3CN(P(OCH_3)_2)_2)((C_6H_5)_2PCH_2CH_2P(C_6H_5)_2)]ClO_4$ (5). To 15 mL of a dichloromethane solution of 4 (0.20 g, 0.25 mmol) was added 0.03 g (0.25 mmol) of trimethyl phosphite in dichloromethane. The solvent was removed in vacuo and the residue recrystallized from acetone/diethyl ether to afford yellow microcrystals of the product in 88% yield: ^1H NMR ($(CD_3)_2CO$) δ 7.4–7.8 (m, 20 H, C_6H_5), 3.67 (m, 12 H, OCH_3), 3.15 (d, $^3J_{P-H}$ = 11.2 Hz, 9 H, $P(OCH_3)_3$), 2.81 (t, $^3J_{P-H}$ = 10.6 Hz, NCH_3); $^{31}P\{^1H\}$ NMR ($(CD_3)_2CO$, 248 K) $\delta(P(= P(OMe)_3))$ 137.9, $\delta(P'(= MeN(P(OMe)_2)_2))$ 104.3, $\delta(P''(= DPPE))$ 59.3 ($J_{P-P'}$ = 108.4, $J_{P-P''}$ = 25.0, $J_{P'-P''}$ = 135.0, $^1J_{Rh-P}$ = 217.9, $^1J_{Rh-P'}$ = 166.0, $^1J_{Rh-P''}$ = 109.1 Hz). Anal. Calcd for $C_{34}H_{48}P_5O_{11}NClRh$: C, 43.44; H, 5.16. Found: C, 41.4; H, 5.2.

$[Rh(CO)(H_3CN(P(OCH_3)_2)_2)((C_6H_5)_2PCH_2CH_2P(C_6H_5)_2)]ClO_4$ (6). Passage of carbon monoxide through an acetone solution of 4 resulted in a color change from yellow to pale yellow-green. Dilution with hexane afforded the product as pale yellow microcrystals in high yield. The complex tends to lose carbon monoxide even in the solid state, and consequently satisfactory elemental analyses could not be obtained: IR 1990 (s) cm^{-1} ($\nu_{C\equiv O}$); $^{31}P\{^1H\}$ NMR ($(CD_3)_2CO$, 248 K) δ 104.6 (m), 59.2 (m).

$[Rh_2(H_3CN(P(OCH_3)_2)_2)_2(\mu\text{-}(C_6H_5)_2PC_4H_2OP(C_6H_5)_2)_2](ClO_4)_2$ (7). $[Rh_2(COD)_2(\mu\text{-}Ph_2PC_4H_2OPPh_2)_2](ClO_4)_2$ was prepared by the same procedure used for $[Rh_2(NBD)_2(\mu\text{-}Ph_2PC_4H_2OPPh_2)_2](BF_4)_2$,[10] and a dichloromethane solution (ca. 15 mL) of the complex (0.20 g, 0.13 mmol) was treated with carbon monoxide to remove the COD. Subsequent dropwise addition of $MeN(P(OMe)_2)_2$ (2 equiv) caused the evolution of gas and change in the color of the solution from yellow to orange-yellow. Removal of the solvent in vacuo followed by washing with diethyl ether gave a yellow powder. This was dissolved in acetone and filtered, and upon dilution of the filtrate with diethyl ether the product precipitated as large yellow flakes in 60% yield. It was characterized by ^1H and ^{31}P NMR spectroscopy: ^1H NMR (CD_2Cl_2) δ 7.3–7.7 (m, 20 H, C_6H_5), 6.19 (s, 2 H, C_4H_2O), 3.41–3.49 (m, 12 H, OCH_3), 2.38 (t, $^3J_{P-H}$ = 10.8 Hz, 3 H, NCH_3); $^{31}P\{^1H\}$ NMR (CD_2Cl_2) $\delta(P_A)$ 102.7, $\delta(P_M)$ 14.8 (AA′MM′X (X = Rh), $J_{A-A'}$ = −32.6, $J_{A-M} = J_{A'-M'}$ = −56.4, $J_{A-M'} = J_{A'-M}$ = 393.5, $J_{M-M'}$ = 68.4, $J_{A-X} = J_{A'-X}$ = 191.4, $J_{M-X} = J_{M'-X}$ = 129.7 Hz).

$[Ir_2(H_3CN(P(OCH_3)_2)_2)_2(\mu\text{-}(C_6H_5)_2PC_4H_2OP(C_6H_5)_2)_2](ClO_4)_2$ (8). To an acetone suspension of $[Ir_2(COD)_2(\mu\text{-}Ph_2PC_4H_2OPPh_2)_2](ClO_4)_2$[15] (0.54 g, 0.31 mmol) was added

---

[7] Kauffman, G. B.; Myers, R. D. *Inorg. Synth.* **1978**, *18*, 131.

[8] Goldschmidt, S.; Krauss, H.-L. *Liebigs Ann. Chem.* **1955**, *595*, 193.

[9] Bishop, J. J.; Davidson, A.; Katcher, M. L.; Lichtenberg, D. W.; Merrill, R. E.; Smart, J. C. *J. Organomet. Chem.* **1971**, *27*, 241.

[10] Brown, J. M.; Canning, L. R. *J. Chem. Soc., Chem. Commun.* **1983**, 460.

[11] Crabtree, R. H.; Quirk, J. M.; Felkin, H.; Fillebeen-Khan, T. *Synth. React. Inorg. Met.-Org. Chem.* **1982**, *12*, 407.

[12] Schrock, R. R.; Osborn, J. A. *J. Am. Chem. Soc.* **1971**, *93*, 3089.

[13] King, R. B. *Organometallic Syntheses*; Academic: New York, 1965; Vol. 1, p 132.

[14] Key to NMR peak multiplicities: s, singlet; d, doublet; t, triplet; q, quintet; dd, doublet of doublets, dquin, doublet of quintets; dq, quintet of doublets; m, multiplet; br, broad.

dropwise 0.15 g (0.70 mmol) of MeN(P(OMe)$_2$)$_2$. The red solid soon dissolved to give a clear yellow solution from which the product crystallized as yellow flakes on dilution with diethyl ether (yield 65%). It was characterized by ^{1}H and ^{31}P NMR spectroscopy: ^{1}H NMR (CD$_2$Cl$_2$) δ 7.3–7.8 (m, 20 H, C$_6$H$_5$), 6.22 (s, 2 H, C$_4$H$_2$O), 3.43–3.50 (m, 12 H, OCH$_3$), 2.31 (t, $^3J_{\mathrm{P-H}}$ = 11.1 Hz, 3 H, NCH$_3$); ^{31}P{^{1}H} NMR (CD$_2$Cl$_2$) δ(P$_\mathrm{A}$) 84.8, δ(P$_\mathrm{X}$) 9.7 (AA′XX′, $J_{\mathrm{A-A'}}$ = 25.9, $J_{\mathrm{A-X}} = J_{\mathrm{A'-X'}}$ = −43.2, $J_{\mathrm{A-X'}} = J_{\mathrm{A'-X}}$ = 394.8, $J_{\mathrm{X-X'}}$ = −36.3 Hz).

[Rh$_2$(H$_3$CN(P(OCH$_3$)$_2$)$_2$)$_4$](O$_3$SCF$_3$)$_2$ (9). A mixture of 0.051 g (0.10 mmol) of [RhCl(COD)]$_2$ and 0.052 g (0.20 mmol) of silver trifluoromethanesulfonate in 10 mL of acetone was stirred for 0.5 h and filtered through a pad of diatomaceous earth to remove the precipitated silver chloride. Addition of 0.089 g (0.40 mmol) of MeN(P(OMe)$_2$)$_2$ to the yellow filtrate caused a color change to a deep magenta. Dilution with diethyl ether formed magenta crystals in virtually quantitative yield: ^{1}H NMR (CD$_2$Cl$_2$) δ 5.57–5.71 (m, 48 H, OCH$_3$), 4.82 (t, $^3J_{\mathrm{P-H}}$ = 6.0 Hz, 6 H, NCH$_3$), 4.56 (t, $^3J_{\mathrm{P-H}}$ = 10.0 Hz, 6 H, NCH$_3$). Anal. Calcd for C$_{22}$H$_{60}$P$_8$O$_{22}$N$_4$F$_6$S$_2$Rh$_2$: C, 19.36; H, 4.44; N, 4.11. Found: C, 19.2; H, 4.4; N, 4.0.

[Ir(H$_3$CN(P(OCH$_3$)$_2$)$_2$)(P(C$_6$H$_5$)$_3$)$_2$]ClO$_4$ (10). To 0.398 g (0.430 mmol) of [Ir(COD)(PPh$_3$)$_2$]ClO$_4$ dissolved in 20 mL of acetone was added dropwise a toluene solution of 0.093 g (0.430 mmol) of MeN(P(OMe)$_2$)$_2$. The initial dark red solution lightened during the addition and at the end had become pale yellow. On stirring the color changed slowly to an orange yellow, and after 15 h the solution was concentrated to ca. 5 mL under reduced pressure. Addition of diethyl ether produced a flocculent orange yellow precipitate. This was filtered off and washed first with diethyl ether containing a little acetone and then with diethyl ether. Recrystallization from acetone/diethyl ether/hexane afforded the product as fluffy orange yellow microcrystals in 75% yield: ^{1}H NMR ((CD$_3$)$_2$CO) δ 7.2–7.6 (m, 30 H, C$_6$H$_5$), 3.58 (m, 12 H, OCH$_3$), 2.43 (t, $^3J_{\mathrm{P-H}}$ = 11.1 Hz, 3 H, NCH$_3$); ^{31}P{^{1}H} NMR ((CD$_3$)$_2$CO) δ(P$_\mathrm{A}$) 84.8, δ(P$_\mathrm{X}$) 20.8 (AA′XX′, $J_{\mathrm{AA'}}$ = 36.5, $J_{\mathrm{XX'}}$ = −25.0, J_{AX} = −44.6, $J_{\mathrm{AX'}}$ = 387.5 Hz). Anal. Calcd for C$_{41}$H$_{45}$P$_4$O$_8$NClIr: C, 47.74; H, 4.41. Found: C, 47.4; H, 4.5.

[Ir(H$_3$CN(P(OCH$_3$)$_2$)$_2$)$_2$(P(C$_6$H$_5$)$_3$)]ClO$_4$ (11). To 0.398 g (0.430 mmol) of [Ir(COD)(PPh$_3$)$_2$]ClO$_4$ in 20 mL of acetone was added dropwise a toluene solution of 0.233 g (1.08 mmol) of MeN(P(OMe)$_2$)$_2$. Dilution of the resulting pale yellow solution with diethyl ether precipitated off-white crystals that were filtered off and washed with diethyl ether. Recrystallization from acetone/diethyl ether/hexane provided a pure sample of the product as very pale yellow crystals in 80% yield: ^{1}H NMR ((CD$_3$)$_2$CO) δ 7.4–7.7 (m, 15 H, C$_6$H$_5$), 3.56 (br, 24 H, OCH$_3$), 2.65 (qd, $J_{\mathrm{P-H}}$ = 5.7, $J_{\mathrm{P'-H}}$ = 1.0 Hz, 6 H, NCH$_3$); ^{31}P{^{1}H} NMR ((CD$_3$)$_2$CO) δ(P) 61.7 (d), δ(P′) 2.2 (q) ($J_{\mathrm{P-P'}}$ = 23.4 Hz). Anal. Calcd for C$_{28}$H$_{45}$P$_5$O$_{12}$N$_2$ClIr: C, 34.17; H, 4.62. Found: C, 33.8; H, 4.64.

[Ir(H$_3$CN(P(OCH$_3$)$_2$)$_2$)(CO)(P(C$_6$H$_5$)$_3$)$_2$]ClO$_4$ (12). A toluene solution of 0.164 g (0.763 mmol) of MeN(P(OMe)$_2$)$_2$ was added dropwise to 0.687 g (0.763 mmol) of [Ir(CO)$_3$(PPh$_3$)$_2$]ClO$_4$ dissolved in a minimum volume of acetone. Gas evolution occurred as the nearly colorless solution took on a definite yellow color. When all the ligand has been added, the solution was sitrred under reduced pressure for several minutes and then under dinitrogen overnight. A small amount of yellow solid was removed by filtration and the filtrate diluted with diethyl ether and hexane to precipitate the product as pale yellow crystals. These were filtered off, washed with diethyl ether, and dried in vacuo (yield 73%): IR 1969 (s) cm^{-1} ($\nu_{\mathrm{C{\equiv}O}}$); ^{1}H NMR ((CD$_3$)$_2$CO) δ 7.1–7.6 (m, 30 H, C$_6$H$_5$), 3.51 (m, 12 H, OCH$_3$), 2.85 (t, $^3J_{\mathrm{P-H}}$ = 11.6 Hz, 3 H, NCH$_3$); ^{31}P{^{1}H} NMR ((CD$_3$)$_2$CO) δ(P) 53.9 (t), δ(P′) 0.3 (t) ($J_{\mathrm{P-P'}}$ = 87.5 Hz). Anal. Calcd for C$_{42}$H$_{45}$P$_4$O$_9$NClIr: C, 47.61; H, 4.29. Found: C, 48.4; H, 4.3.

[Ir(c-C$_8$H$_{12}$)((η^5-C$_5$H$_4$P(C$_6$H$_5$)$_2$)$_2$Fe)]ClO$_4$ (13). A mixture of 0.149 g (0.719 mmol) of AgClO$_4$ and 0.241 g (0.359 mmol) of [IrCl(COD)]$_2$ in 15 mL of acetone was stirred at room temperature for 2 h and the precipitated silver chloride removed by filtration through a pad of diatomaceous earth. To the filtrate was added dropwise a solution of 0.399 g (0.719 mmol) of BDPPF in the minimum volume of dichloromethane. The solution rapidly became dark red, and toward the end of the addition 10 mL more dichloromethane was added to the reaction mixture to keep the product in solution. The final reaction mixture was stirred for 4 h and concentrated to ca. 15 mL under reduced pressure whereupon the product began to crystallize. Addition of diethyl ether completed the precipitation, and the dark purple-red crystals were filtered off, washed with diethyl ether, and dried in vacuo (yield 90%): ^{1}H NMR ((CD$_3$)$_2$CO) δ 7.6–8.1 (m, 20 H, C$_6$H$_5$), 4.45–4.49 (m, 8 H, cyclopentadienyl), 4.20 (br, 4 H), 1.9–2.5 (m, 8 H) (COD); ^{31}P{^{1}H} NMR ((CD$_3$)$_2$CO) δ 15.7 (s). Anal. Calcd for C$_{42}$H$_{40}$O$_4$P$_2$ClFeIr: C, 52.86; H, 4.23. Found: C, 52.2; H, 4.6.

[Ir(H$_3$CN(P(OCH$_3$)$_2$)$_2$)((η^5-C$_5$H$_4$P(C$_6$H$_5$)$_2$)$_2$Fe)]ClO$_4$ (14). To 20 mL of a solution of 0.323 g (0.339 mmol) of [Ir(COD)(BDPPF)]ClO$_4$ in acetone/dichloromethane (1:1, v:v) was added dropwise a toluene solution of 0.080 g (0.373 mmol) of MeN(P(OMe)$_2$)$_2$. The resulting orange solution was stirred overnight and then concentrated to approximately half the original volume under reduced pressure. Addition of diethyl ether and hexane precipitated the product that was filtered off, washed with diethyl ether, and recrystallized from acetone/dichloromethane/diethyl ether/hexane to yield orange-brown crystals (80%): ^{1}H NMR (CD$_2$Cl$_2$) δ 7.4–8.0 (m, 20 H, C$_6$H$_5$), 4.25–4.36 (m, 8 H, cyclopentadienyl), 3.40 (m, 12 H, OCH$_3$), 2.26 (t, $^3J_{\mathrm{P-H}}$ = 11.0 Hz, 3 H, NCH$_3$); ^{31}P{^{1}H} NMR (CD$_2$Cl$_2$) δ(P$_\mathrm{A}$) 87.0, δ(P$_\mathrm{X}$) 19.0 (AA′XX′, $J_{\mathrm{AA'}}$ = 33.9, $J_{\mathrm{XX'}}$ = −25.9, J_{AX} = −44.0, $J_{\mathrm{AX'}}$ = 398.5 Hz). Anal. Calcd for C$_{39}$H$_{43}$P$_4$O$_8$NClFeIr: C, 44.14; H, 4.09. Found: C, 43.8; H, 4.4.

[Ir(H$_3$CN(P(OCH$_3$)$_2$)$_2$)$_3$]ClO$_4$ (15). A mixture of 0.149 g (0.718 mmol) of silver perchlorate and 0.241 g (0.359 mmol) of [IrCl(COD)]$_2$ in 20 mL of acetone was stirred for 2 h at room temperature and filtered through a pad of diatomaceous earth to remove the precipitated silver chloride. To the filtrate was added dropwise 0.463 g (2.154 mmol) of MeN(P(OMe)$_2$)$_2$. The solution became very dark and, as the addition was continued, turned to a bright emerald green. At the end it was a medium yellow and after about 1.5 h had become pale yellow. After being stirred overnight the solution was diluted with diethyl ether to the cloud point and cooled in a freezer whereupon an oil formed. Considerable effort to obtain a solid product was unsuccessful, and the crude oil was characterized by ^{31}P NMR spectroscopy (see Results and Discussion).

X-ray Crystallography. Very pale yellow crystals of **12** were grown by slow diffusion of diethyl ether into an acetone solution of the complex. An approximately rectangular plate was cut from a clump of crystals and mounted in a thin-walled capillary on an Enraf-Nonius CAD-4 diffractometer. Cell constants and an orientation matrix for the data collection were obtained from a least-squares refinement of the setting angles of 25 high-order reflections that had been accurately centered by using the CAD-4 software. The space group was determined from the systematic absences apparent in the final data set and was confirmed by the successful refinement. Intensity data were collected by using the parameters given in Table I, and an attenuator was automatically inserted in front of the detector for intense reflections. Three check reflections were measured every 2 h and showed a slight (1.2%) linear decrease in intensity over the period of the data collection. The raw intensities were corrected for Lorentz and polarization effects, the decrease in intensity of the standards and for absorption based on psi scans for 9 reflections having χ in the range 82–90°. Equivalent reflections were averaged resulting in an agreement factor of 0.02 based on F. The structure was solved by direct methods (MULTAN) and refined by full-matrix least squares using unit weights.[16] It soon became evident that the perchlorate ion was affected by disorder. Thus while two oxygen atoms (O$_2$, O$_3$) appeared well-behaved, the electron density due to the others was significantly smeared out in an arc on the other side of the chlorine atom. This suggested several orientations of the ion that are related by a rocking about the O$_2$–O$_3$ axis and implies the chlorine atom occupies substantially overlapping sites. These could not be distinguished so a single chlorine atom was retained. This refined satisfactorily, but its disorder is reflected in the rather elongated thermal ellipsoid that resulted. From a

---

(15) Brown, J. M.; Canning, L. R.; Lucy, A. R. *J. Chem. Soc., Chem. Commun.* **1984**, 915.

(16) All calculations were carried out on a PDP 11-73 computer using the Enraf-Nonius SDP set of programs. Atom scattering factors were corrected for the effects of anomalous dispersion.

Table I. Crystal and Intensity Collection Data for 9 and 12

	9	12
formula	$C_{22}H_{60}P_8O_{22}N_4F_6S_2Rh_2$	$C_{42}H_{45}P_4O_9NClIr$
fw	1364.56	1059.43
cryst system	monoclinic	monoclinic
space group	$P2_1/c$	$P2_1/c$
a, Å	22.676 (4)	16.067 (2)
b, Å	19.079 (4)	14.421 (2)
c, Å	12.236 (7)	19.574 (4)
β, deg	97.12 (3)	102.49 (1)
V, Å^3	5253	4427
Z	4	4
ρ(calcd), g cm^{-3}	1.72	1.59
radiatn	Mo Kα, graphite monochromated, λ = 0.710 73 Å	
linear abs coeff, cm^{-1}	10.2	32.6
trans factor range	0.80–1.0	0.77–1.0
θ range, deg	0.5–24.5	1–25
scan type	ω–2θ	ω–2θ
scan width, deg	0.80 + 0.20 tan θ	0.75 + 0.34 tan θ
scan rate, deg min^{-1}	1.6–16.5	1.6–16.5
atten factor	11.84	11.84
programs used	Enraf-Nonius SDP	Enraf-Nonius SDP
p factor in weight	0.04	0.04
unique data	8729	7769
data with I > 3.0*(I)	6097	5462
no. of variables	523	341
largest shift/esd in final cycle	0.05[e]	0.11[a]
R[b]	0.055	0.037
R_w[c]	0.082	0.048
goodness of fit[d]	2.66	1.52

[a] Excluding disordered atoms. [b] $R = \sum||F_o| - |F_c||/\sum|F_o|$. [c] $R_w = [\sum w(|F_o - F_c|)^2/\sum w(|F_o|)^2]^{1/2}$. [d] $\mathrm{GOF} = [\sum w(|F_o| - |F_c|)^2/(N_o - N_v)]^{1/2}$, where N_o and N_v are the number of observations and variables, respectively. [e] Excluding the trifluoromethyl group. Mo Kα, graphite monochromated, λ = 0.710 73 Å

difference Fourier map phased on all atoms but the disordered oxygens, two reasonable alternate sites could be chosen for them and the occupancy of each was fixed at 50%. Refinement of the disordered oxygen atoms with isotropic thermal parameters proceeded adequately but even at the end the shift/error values for these atoms were significantly larger (0.5–1.9) than for the rest. Also the final difference map showed residual electron density between the disordered atoms. It is clear that the model used is not totally satisfactory, but in light of the low value for R and the fact that the perchlorate ion is such a small portion of the structure further effort does not appear to be justified. In the final stages of the refinement, the hydrogen atoms of the phenyl groups were included in calculated positions (C–H = 0.95 Å) with isotropic thermal parameters 1.3 times that of the attached carbon atom. These were not refined but were reset after every second cycle of refinement. Also the weighting scheme was changed to one where $w = 1/\sigma_F^2$ ($\sigma_F = \sigma_{F^2}/2F$ and $\sigma_{F^2} = (\sigma_I^2 + (0.04F^2)^2)^{1/2}$. The final difference Fourier showed only small features (ca. ±0.8 e/A^3) that could be attributed either to hydrogen atoms of the methyl groups or to the residual disorder of the perchlorate ion. Final positional parameters are given in Table II, and additional crystallographic data included as supplementary material.

Table II. Positional Parameters for $[Ir(CO)(MeN(P(OMe)_2)_2)(PPh_3)_2]ClO_4$

atom	x	y	z	B, Å^2
Ir	0.22346 (2)	0.17880 (2)	0.33942 (1)	2.391 (4)
P1	0.2730 (1)	0.3361 (1)	0.3372 (1)	3.10 (4)
P2	0.3330 (1)	0.0975 (1)	0.30158 (9)	2.72 (4)
P3	0.1183 (1)	0.1259 (1)	0.2507 (1)	3.20 (4)
P4	0.0920 (1)	0.2199 (1)	0.3554 (1)	3.17 (4)
C1	0.2607 (4)	0.1320 (5)	0.4318 (4)	3.3 (2)
O1	0.2774 (4)	0.1044 (4)	0.4873 (3)	4.9 (1)
N	0.0378 (4)	0.1662 (4)	0.2845 (3)	3.7 (1)
C2	−0.0566 (5)	0.1582 (7)	0.2595 (5)	5.5 (2)
O31	0.0950 (3)	0.0205 (3)	0.2326 (3)	4.0 (1)
C31	0.0873 (6)	−0.0432 (6)	0.2893 (5)	5.3 (2)
O32	0.1094 (3)	0.1632 (4)	0.1734 (3)	4.4 (1)
C32	0.0397 (6)	0.1393 (8)	0.1133 (5)	6.5 (3)
O41	0.0613 (3)	0.3237 (3)	0.3511 (3)	4.2 (1)
C41	0.0050 (6)	0.3678 (7)	0.3901 (5)	6.1 (2)
O42	0.0570 (3)	0.1873 (4)	0.4212 (3)	5.0 (1)
C42	0.0575 (6)	0.0940 (7)	0.4455 (5)	6.5 (2)
Cl	0.8526 (2)	0.3179 (2)	0.0333 (1)	6.50 (6)
O2	0.8683 (7)	0.2792 (6)	0.0994 (4)	11.1 (3)
O3	0.8681 (7)	0.2647 (7)	−0.0184 (5)	14.6 (3)
O4A	0.928 (1)	0.378 (1)	0.0411 (9)	10.2 (5)*
O4B	0.853 (1)	0.408 (1)	0.026 (1)	11.2 (5)*
O5A	0.794 (1)	0.395 (1)	0.0274 (8)	8.8 (4)*
O5B	0.759 (1)	0.292 (1)	0.020 (1)	11.4 (5)*
C111	0.3884 (5)	0.3578 (5)	0.3616 (4)	3.5 (1)*
C112	0.4275 (5)	0.3855 (6)	0.4295 (4)	4.5 (2)*
C113	0.5155 (6)	0.3938 (7)	0.4497 (5)	6.0 (2)*
C114	0.5648 (6)	0.3756 (7)	0.4008 (5)	6.1 (2)*
C115	0.5283 (6)	0.3495 (7)	0.3322 (5)	5.8 (2)*
C116	0.4387 (5)	0.3412 (6)	0.3141 (4)	4.5 (2)*
C121	0.2364 (5)	0.4086 (5)	0.4018 (4)	3.6 (1)*
C122	0.2323 (5)	0.3736 (6)	0.4660 (4)	4.4 (2)*
C123	0.2102 (6)	0.4274 (6)	0.5189 (5)	5.6 (2)*
C124	0.1884 (6)	0.5197 (7)	0.5037 (5)	6.3 (2)*
C125	0.1909 (6)	0.5565 (7)	0.4399 (5)	6.1 (2)*
C126	0.2158 (5)	0.5020 (6)	0.3892 (4)	4.6 (2)*
C131	0.2407 (5)	0.4043 (5)	0.2562 (4)	3.8 (1)*
C132	0.1641 (5)	0.3828 (6)	0.2124 (4)	4.3 (2)*
C133	0.1345 (6)	0.4317 (7)	0.1503 (5)	5.8 (2)*
C134	0.1842 (6)	0.5025 (7)	0.1343 (5)	6.1 (2)*
C135	0.2573 (6)	0.5268 (7)	0.1761 (5)	5.9 (2)*
C136	0.2885 (5)	0.4773 (6)	0.2383 (4)	4.9 (2)*
C211	0.4324 (4)	0.0797 (5)	0.3652 (4)	3.1 (1)*
C212	0.4579 (5)	0.1430 (5)	0.4185 (4)	3.8 (1)*
C213	0.5386 (5)	0.1351 (6)	0.4640 (4)	4.6 (2)*
C214	0.5916 (5)	0.0646 (6)	0.4557 (4)	4.6 (2)*
C215	0.5659 (5)	0.0002 (6)	0.4038 (4)	4.9 (2)*
C216	0.4870 (5)	0.0064 (5)	0.3585 (4)	4.0 (2)*
C221	0.3671 (5)	0.1459 (5)	0.2249 (4)	3.4 (1)*
C222	0.4459 (6)	0.1241 (7)	0.2105 (5)	5.8 (2)*
C223	0.4689 (8)	0.1697 (8)	0.1532 (6)	7.5 (3)*
C224	0.4157 (6)	0.2290 (7)	0.1128 (5)	6.3 (2)*
C225	0.3373 (6)	0.2488 (6)	0.1246 (5)	5.1 (2)*
C226	0.3129 (5)	0.2061 (5)	0.1823 (4)	3.8 (1)*
C231	0.3026 (4)	−0.0215 (5)	0.2752 (4)	3.2 (1)*
C232	0.2802 (5)	−0.0485 (5)	0.2058 (4)	4.1 (2)*
C233	0.2563 (6)	−0.1399 (6)	0.1888 (5)	5.0 (2)*
C234	0.2590 (6)	−0.2034 (6)	0.2396 (5)	5.5 (2)*
C235	0.2794 (6)	−0.1803 (6)	0.3087 (5)	5.7 (2)*
C236	0.3023 (5)	−0.0862 (6)	0.3272 (4)	4.6 (2)*

[a] Parameters with an asterisk were refined isotropically. Anisotropically refined atoms are given in the form of the isotropic equivalent displacement parameter defined as $(^4/_3)[a^2B(1,1) + b^2B(2,2) + c^2B(3,3) + ab(\cos\gamma)B(1,2) + ac(\cos\beta)B(1,3) + bc(\cos\alpha)B(2,3)]$.

Burgundy crystals of 9 were grown by slow diffusion of diethyl ether into an acetone solution of the complex. A thin plate was chosen and mounted in a thin-walled capillary on an Enraf-Nonius CAD-4 diffractometer. Unit cell and space group determinations as well as the data collection proceeded as described for 12, and specific details appear in Table I. Data reduction and correction also was performed similarly (agreement factor on F for averaged reflections was 0.014). In this instance, the three standards showed an anisotropic decrease in intensity which averaged 9.9%. An appropriate correction was made. Solution and initial refinement of the structure proceeded as described for 12. Following location and isotropic refinement of all non-hydrogen atoms of the cation and one trifluoromethanesulfonate anion, a difference map indicated substantial disorder of the second anion. After considerable trial and error, a model consisting of three different orientations (A, B, and C) of an approximately idealized trifluoromethanesulfonate ion with occupancies of 0.50 (A), 0.35 (B), and 0.15 (C) and isotropic thermal parameters equal to those for the corresponding atoms (averaged values for oxygen and fluorine) of the ordered anion was adopted. This model was held fixed, and the ordered atoms were refined anisotropically to near convergence. Further refinement to near convergence with weights set equal to $1/\sigma_F^2$ (defined as for 12) was followed by a separate refinement (one cycle each) of the positional parameters of each orientation of the disordered anion. A second cycle of refinement of each of the orientations A and B produced a difference map suggesting the occupancies should be 0.48 (A), 0.32 (B), and 0.20 (C). These and the partially refined positional parameters then were fixed for the remainder of the refinement. Although the limited refinement of the disordered anion resulted in some noticeable departure from idealized geometry, the resulting diminution of the residual features in the difference map in this region suggests that the final model obtained is preferable to the initial idealized one. At this point, a sufficient number of hydrogen atoms could be located to enable all hydrogen atoms except those associated with C_{51} and C_{81} to be placed in idealized positions (C–H = 0.95 Å). There were included as fixed contributions with isotropic thermal parameters equal to 1.3 times the equivalent isotropic thermal parameters of the attached carbon atom and were periodically updated. The final difference map showed features ranging from 1.04 to −1.39 e/Å^3. The largest of these were associated with the disordered anion, indicating the disorder has not been fully modeled. However in view of the reasonable value obtained for *R*, further effort to better model the disorder does not seem to be worthwhile. Elsewhere, residual features in the map are no more than ±0.7 e/Å^3. In the final cycle, the largest shift/esd was 0.48, which is associated with the carbon atom of the ordered anion. The larger thermal ellipsoids for this trifluoromethyl group and the oscillating parameter shifts indicate a small degree of disorder here too. Final positional parameters are given in Table V, and additional crystallographic data are included as supplementary material.

Results and Discussion

Synthesis of Compounds. Reaction of $PhN(P(OMe)_2)_2$ with $[Rh(COD)(acetone)_x]ClO_4$ using ligand/metal ratios of 1, 2, or 3 forms complexes analyzing as $[Rh(COD)(PhN(P(OMe)_2)_2]ClO_4$ (**1**), $[Rh(PhN(P(OMe)_2)_2)_2]ClO_4$ (**2**), and $[Rh_2(PhN(P(OMe)_2)_2)_5](ClO_4)_2$ (**3**), respectively, the last being isolated as an acetone solvate. As noted in the Experimental Section, initial contact of the ligand with the $[Rh(COD)(acetone)_x]ClO_4$ generates a magenta-colored solution which rapidly fades to the yellow orange of the isolated products. If the reaction leading to **2** is performed at −78 °C, a magenta product can be isolated at this temperature that analyzes as $[Rh(PhN(P(OMe)_2)_2)_2]ClO_4$[17] but is clearly different from **2**. Although its instability in solution precluded spectroscopic characterization, its color is essentially the same as that of $[Rh_2(MeN(P(OMe)_2)_2)_2(\mu\text{-}MeN(P(OMe)_2)_2)_2](CF_3SO_3)_2$ (**9**, vide infra) and we therefore assign it an analogous structure.

The NMR data for **1** and **2** are consistent with their formulation as monomeric, square-planar complexes containing chelating $PhN(P(OMe)_2)_2$ ligands. Chelation is indicated by the significant upfield shift of the ^{31}P resonances from the free-ligand values which is consistent with the formation of a four-membered chelate ring.[18] In **1** the resonance due to the methoxy protons appears as a characteristic "virtually coupled" multiplet, but somewhat surprisingly in **2** only a broad peak is seen. The $^{31}P\{^1H\}$ NMR spectrum of **3** consists of a doublet of doublets well upfield and a doublet of quintets slightly downfield of the chemical shift of the free ligand. The 4:1 intensity ratio and the chemical shifts indicate that the former is due to two chelating ligands while the latter is due to a nonchelating ligand with both ends equivalently coordinated. The complex is therefore formulated as $[Rh_2(PhN(P(OMe)_2)_2)_4(\mu\text{-}PhN(P(OMe)_2)_2)](ClO_4)_2$, and the data are in accord with either square-pyramidal coordination about rhodium with the bridging ligand connecting apical sites or with a fluxional trigonal-bipyramidal coordination with the bridging ligand connecting equatorial sites. As the ^{31}P NMR spectrum is little different at 228 K than at room temperature, no firm choice can be made but we favor the latter for the following reasons. First, the related complex $[Rh(P(OMe)_3)_5]BPh_4$ and several analogues have been shown to adopt trigonal-bipyramidal structures and to be highly fluxional.[19,20] In addition, the coordination chemical shift (ca. 4 ppm downfield) and rhodium–phosphorus coupling constant for the equatorial ligands in $[Rh(P(OMe)_3)_5]BPh_4$ compare well with those assigned to the bridging ligand in **3** while the (average) rhodium–phosphorus coupling to the chelate ligand is not too different from that reported for $^1J_{Rh-P}$ for the axial ligands in $[Rh(P(OMe)_3)_5]BPh_4$.[20] On cooling to 228 K no significant change in the appearance of the spectrum occurred, but the chemical shift of the chelate ligands moves downfield by ca. 3 ppm and the apparent phosphorus–phosphorus coupling constant between the chelate and bridging ligands decreases by 5.5 Hz. This behavior would seem to be more consistent with a fluxional molecule, and it might be noted that the temperature of 228 K, which was the lowest at which we could obtain a satisfactory spectrum, is well above that at which noticeable differences from the fast-exchange spectrum were seen for $[Rh(P(OMe)_3)_5]BPh_4$ (ca. 182 K).[19,20] The proposed structure is also that reported for $[Fe_2(dmpe)_4(\mu\text{-}dmpe)]$ (dmpe = 1,2-bis(dimethylphosphino)ethane).[21]

Reaction of slightly more than 1 equiv of $MeN(P(OMe)_2)_2$ with $[Rh(COD)(DPPE)]ClO_4$ forms $[Rh(MeN(P(OMe)_2)_2)(DPPE)]ClO_4$ (**4**) which is formulated as a square-planar species on the basis of the analytical and spectroscopic data. This readily forms five-coordinate adducts with trimethyl phosphite and carbon monoxide that are formulated as $[Rh(L)(MeN(P(OMe)_2)_2)(DPPE)]ClO_4$ (L = $P(OMe)_3$ (**5**), CO (**6**)). The presence of a carbonyl ligand in **6** is confirmed by the appearance of a band attributable to ν_{CO} at 1990 cm^{-1}, but as this disappears on flushing, the solution with dinitrogen the complex is evidently not very stable. Carbon monoxide loss also occurs more slowly in the solid state as evidenced by a slow change in color from the pale yellow of **6** to the yellow orange of **4**. Although not conclusive, ^{31}P NMR spectra of **5** in the presence of added trimethyl phosphite suggest that exchange of free and coordinated phosphite occurs. In the absence of added trimethyl phosphite, the ^{31}P NMR spectrum of **5** shows three rather poorly resolved resonances at room temperature, but at 248 K a satisfactory spectrum was obtained that showed no further change on cooling to 208 K. This can be readily interpreted if magnetic equivalence of each end of each chelate ligand is assumed.[22] Again this is consistent either with a square-pyramidal geometry and an apical trimethyl phosphite ligand or with a fluxional trigonal-bipyramidal structure in which the trimethyl phosphite occupies an equatorial site. No choice can be made on the basis of the available data, but as has been argued earlier, the latter is preferred.

In an attempt to prepare an oligomeric species with alternating short and long metal–metal distances, the complexes $[M_2(COD)_2(\mu\text{-}Ph_2PC_4H_2OPPh_2)_2](ClO_4)_2$ (M =

---

[17] Calcd for $C_{20}H_{34}P_4O_{12}N_2ClRh$: C, 31.76; H, 4.49; N, 3.70. Found: C, 31.1; H, 4.7; N, 3.2.

[18] Garrou, P. E. *Chem. Rev.* 1981, *81*, 229.

[19] Meakin, P.; Jesson, J. P. *J. Am. Chem. Soc.* 1973, *95*, 7272.

[20] Meakin, P.; Jesson, J. P. *J. Am. Chem. Soc.* 1974, *96*, 5751.

[21] Tolman, C. A.; Ittel, S. D.; English, A. D.; Jesson, J. P. *J. Am. Chem. Soc.* 1978, *100*, 4080.

[22] An excellent simulation of the spectrum to give the parameters listed in the Experimental Section can be achieved if an A_2M_2XZ (A, $MeN(\mathit{P}(OMe)_2)_2$; M, $Ph_2\mathit{P}CH_2CH_2\mathit{P}Ph_2$; X, $\mathit{P}(OMe)_3$; Z, *Rh*) spin system is used.

Rh, Ir) were treated with 2 equiv of $MeN(P(OMe)_2)_2$ to afford products analyzing as $[M(MeN(P(OMe)_2)_2)(Ph_2PC_4H_2OPPh_2)]ClO_4$ (M = Rh (**7**), Ir (**8**)). From the ^{31}P NMR spectra (**7**, AA'MM'X; **8**, AA'XX') it appears, however, that the $MeN(P(OMe)_2)_2$ ligand chelates to a single metal and the products are formulated as $[M_2(MeN(P(OMe)_2)_2)_2(\mu\text{-}Ph_2PC_4H_2OPPh_2)_2](ClO_4)_2$ with structures that are presumably analogous to those of the starting cyclooctadiene complexes. A second attempt to prepare oligomers from $[Rh_2(COD)_2(\mu\text{-}Ph_2PC_4H_2OPPh_2)_2](ClO_4)_2$ involved reaction with 2 equiv of DPM, but here the product was the known complex $[Rh(DPM)_2]ClO_4$.[23]

Unlike $PhN(P(OMe)_2)_2$, $MeN(P(OMe)_2)_2$ reacts immediately with $[RhCl(COD)]_2$ or $[Rh(COD)(acetone)_x]^+$ with ligand to metal ratios of either 1:1 or 2:1 to form the intensely magenta-colored cation $[Rh_2(MeN(P(OMe)_2)_2)_2(\mu\text{-}MeN(P(OMe)_2)_2)_2]^{2+}$ (**9**) whose structure is shown in Figure 3. Crystalline tetraphenylborate, hexafluorophosphate, perchlorate, and trifluoromethanesulfonate salts could be isolated but only the last afforded X-ray quality crystals. When a 2:1 ratio of ligand to metal is used, **9** forms in high yield while with the 1:1 ratio **9** forms in 50% yield with the remaining rhodium presumably being converted to $[Rh(COD)_2]^+$. The ^{31}P NMR spectrum of **9** consists of several broad resonances in the range δ 90–137. These contain much fine structure and some changes occur on cooling indicating some degree of fluxionality, but because of the complexity an analysis was not feasible. The magenta color of **9** is quite similar to that of $[Rh_2(CN\text{-}t\text{-}Bu)_4(DPM)_2]PF_6$,[24] and, like the isocyanide complex, **9** exhibits a relatively intense (ϵ 8309 M^{-1} cm^{-1}) absorption at 538 nm. The position and intensity of this band together with the observed metal–metal separation of 3.2727 (5) Å indicate it can be assigned to a "proximity-shifted" absorption.[25] Passage of carbon monoxide through a solution of **9** bleaches the color to yellow and carbonyl absorptions appear at 2042 (w), 2014 (w), and 1864 (s) cm^{-1}. Loss of carbon monoxide occurs readily on flushing the solution with dinitrogen. Because of the lability of the carbonyl ligands we were unable to obtain a satisfactory solid product. However, the ^{31}P NMR spectrum obtained in situ at low temperature is quite similar to that of **9** suggesting that the phosphorus ligand framework remains substantially the same. With the limited data available it is uncertain whether or not a single species is formed, but it is clear that a bridging carbonyl ligand is present and in this regard **9** behaves in an analogous fashion to $[Rh_2(CN\text{-}t\text{-}Bu)_4(DPM)_2](PF_6)_2$ which also forms a very labile carbonyl-bridged adduct.[26]

Following several unsuccessful attempts to prepare binuclear iridium(I) complexes of $MeN(P(OMe)_2)_2$ using methods employed for complexes of DPM[27] (vide infra), the ligating behavior of $MeN(P(OMe)_2)_2$ toward iridium(I) species containing a smaller number of readily replaceable ligands was investigated. Reaction of $[Ir(COD)(PPh_3)_2]ClO_4$ with 1 and slightly more than 2 equiv of the ligand forms $[Ir(MeN(P(OMe)_2)_2)(PPh_3)_2]ClO_4$ (**10**) and $[Ir(MeN(P(OMe)_2)_2)_2(PPh_3)]ClO_4$ (**11**), respectively, while equimolar quantities of $[Ir(CO)_3(PPh_3)_2]ClO_4$ and the ligand yield $[Ir(CO)(MeN(P(OMe)_2)_2)(PPh_3)_2]ClO_4$ (**12**).

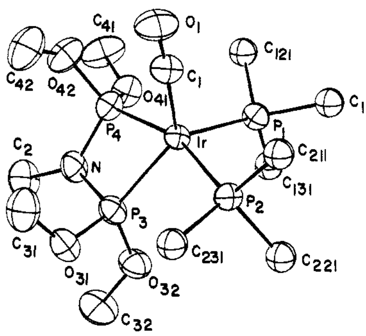

Figure 1. A perspective view of the $[Ir(CO)(MeN(P(OMe)_2)_2)(PPh_3)_2]^+$ cation (**12**). Thermal ellipsoids are drawn at the 50% probability level, and only the quaternary carbon atoms of the phenyl groups are shown. The remaining carbon atoms of these groups are numbered sequentially around each ring with the third digit of the subscript as the running index.

The structure of **12** has been determined by X-ray crystallography and is shown in Figure 1 while the spectroscopic data for **10** are consistent with it being a square-planar species with a chelating $MeN(P(OMe)_2)_2$ ligand. The ^{31}P NMR spectrum of **12** at room temperature consists of two triplets implying two pairs of equivalent phosphorus atoms and thereby indicates the molecule is fluxional. Cooling to 208 K causes the center peak of the upfield triplet and the outer peaks of the downfield triplet to broaden significantly indicating a slowing of the fluxional process, but even here, the spectrum is far from that expected (vide infra) for the static structure that is found in the solid state. This is not surprising since the distortion of the coordination sphere due to the short bite of the chelate ligand (see Figure 1) should render the interconversion of axial and equatorial phosphorus sites quite facile. The room-temperature ^{31}P NMR spectrum of **11** is consistent with either a square-pyramidal (triphenylphosphine apical) or a fluxional trigonal-bipyramidal (triphenylphosphine equatorial) structure. The spectrum remains essentially unchanged on cooling to 208 K although, as noted for **3**, the interligand phosphorus–phosphorus coupling decreases slightly. Since **12** is approximately trigonal-bipyramidal and the majority of five-coordinate, d^8 metal complexes containing only phosphorus ligands appear to have fluxional trigonal-bipyramidal structures[20] as well, we prefer this structure for **11**. Again, the short bite of the chelate ligand should render the barrier to interconversion quite low as has been observed for $[Fe(CO)(DPM)_2]$[23] and $[Ir(CO)(DPM)_2]Cl$.[29] Consistent with the proposed fluxional structure is the observation that the single resonance observed for the methoxy protons of the ligand at room temperature splits into several broad resonances at 208 K.

Reaction of $[Ir(COD)(acetone)_x]ClO_4$ with 1 equiv of 1,1'-bis(diphenylphosphino)ferrocene (BDPPF) readily affords $[Ir(COD)(BDPPF)]ClO_4$ (**13**) which is well-characterized by its spectroscopic data and is analogous to the previously reported $[Ir(COD)(DPPP)]BF_4$[30] (DPPP = 1,3-bis(diphenylphosphino)propane). Addition of 1 equiv of $MeN(P(OMe)_2)_2$ to **13** affords a good yield of a species formulated as $[Ir(MeN(P(OMe)_2)_2)(BDPPF)]ClO_4$ (**14**). Like **10**, **14** exhibits a ^{31}P NMR spectrum that could be successfully analyzed as an AA'XX' spin system indicating a square-planar structure. Complex **14** reacts with dimethyl acetylenedicarboxylate (DMAD), dioxygen, dihydrogen, and iodine, but in no case could a pure product

---

(23) van der Ploeg, A. F. M. J.; van Koten, G. *Inorg. Chim. Acta* **1981**, *51*, 225.

(24) Balch, A. L. *J. Am. Chem. Soc.* **1976**, *98*, 8049.

(25) Balch, A. L.; Tulyathan, B. *Inorg. Chem.* **1977**, *16*, 3840.

(26) Mague, J. T.; DeVries, S. H. *Inorg. Chem.* **1980**, *19*, 3743.

(27) Mague, J. T.; Sanger, A. R. *Inorg. Chem.* **1979**, *18*, 2060.

(28) Ittel, S. D.; Tolman, C. A.; Krusic, P. J.; English, A. D.; Jesson, J. P. *Inorg. Chem.* **1978**, *17*, 3432.

(29) Miller, J. S.; Caulton, K. G. *J. Am. Chem. Soc.* **1975**, *97*, 1067.

(30) Wang, H. H.; Pignolet, L. H. *Inorg. Chem.* **1980**, *19*, 1470.

be obtained. From NMR data, the major component of the powdery product obtained from the first reaction appears to be the expected [Ir(DMAD)(MeN(P(OMe)$_2$)$_2$)(BDPPF)]ClO$_4$ and the ^{31}P NMR spectrum (Figure 4) is consistent with the structure A. Thus four distinct doublets of doublets of doublets having approximately equal intensity are seen which from their chemical shifts and coupling constants can be assigned as follows: $\delta(P_1)$ 33.18 $\delta(P_2)$ 51.6, $\delta(P_3)$ −7.6, $\delta(P_4)$ −5.2 (J_{12} = 24.2, J_{13} = 28.2, J_{14} = 602.5, J_{23} = 32.4, J_{24} = 41.1, J_{34} = 18.8 Hz). The value of J_{14} is one of the largest observed to date for $^2J_{P-P}$ and clearly indicates these two phosphorus atoms must be trans to one another. A puzzling feature of this spectrum is the significantly greater breadth of the components of the multiplet assigned to P$_4$ as compared with the others. On cooling each half of the major doublet broadens into a featureless hump, but the ~600 Hz coupling to P$_1$ appears to be retained and the other multiplets change only slightly in appearance and resolution. A similar spectrum is obtained when a deuteriodichloromethane solution of **14** is flushed with dioxygen although conversion to the presumed dioxygen adduct was incomplete and decomposition soon ensued. With the same labeling as in A one has $\delta(P_1)$ 33.7, $\delta(P_2)$ 43.5, $\delta(P_3)$ −6.4, and $\delta(P_4)$ −4.1 (J_{12} = 14.7, J_{13} = 26.7, J_{14} = 587.6, J_{23} = 5, J_{24} = 13.5, J_{34} = 14.6 Hz). At present we have no adequate explanation for the breadth of the resonance assigned to the axial phosphorus atom of BDPPF.

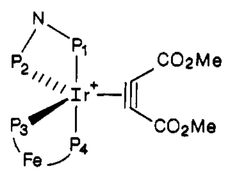

A

The reactions of MeN(P(OMe)$_2$)$_2$ with [IrCl(COD)]$_2$ or [Ir(COD)(acetone)$_x$]ClO$_4$ are complex and appear to be sensitive to the rate of ligand addition. The only well-characterized product is obtained from [Ir(COD)(acetone)$_x$]ClO$_4$ and 3 equiv of the ligand. Concentration of the resulting pale yellow solution and dilution with diethyl ether and/or hexane form a cream-colored oil (**15**) which we were unable to induce to crystallize. The ^{31}P NMR spectrum at 268 K of the crude oil showed one major species having resonances at δ 63.5 (dd), 123.0 (dquin), and 146.7 (dquin)[14] with relative intensities of 4:1:1. The most reasonable formulation is a five-coordinate species with two chelating and one monodentate MeN(P(OMe)$_2$)$_2$ ligands (note the free ligand has δ(P) 146.3) which, following earlier arguments, has a fluxional trigonal-bipyramidal structure. The apparent coupling constants derived from the 268 K spectrum are J_{12} = 56.3, J_{13} = 11.1, and J_{23} = 84.0 Hz with the significant long-range coupling between P$_1$ and P$_3$ being noteworthy. As before, the value of J_{12} decreases slightly while that for J_{13} increases (ca. 10 Hz) on cooling. The latter increase is consistent with a decreasing rate of torsional motion within the monodentate ligand.[31]

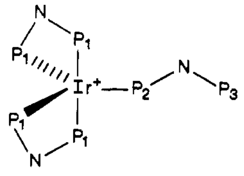

The reaction of [Ir(COD)(acetone)$_x$]ClO$_4$ with 1 equiv of MeN(P(OMe)$_2$)$_2$ added over a period of several minutes is accompanied by color changes from nearly black to bright emerald green to a dark brownish red by the end of the addition of the ligand. The ^{31}P NMR spectrum of the reaction mixture shows resonances at δ 51.8 (s) and 118.7 (s)[14] as the only significant features. Addition of a second equivalent of ligand to this solution at a comparable rate causes a color change to dirty yellow, and the resulting ^{31}P NMR spectrum, obtained within an hour, shows, in addition to the same two singlets, resonances due to **15** and multiplets centered at δ 61.8 and 129.2. After 4 h, the solution becomes somewhat orange in color, and the ^{31}P NMR spectrum now shows that the species responsible for the multiplets at δ 61.8 and 129.2 is the major component while the other resonances observed earlier have disappeared. A series of weak, poorly resolved resonances are also seen in the δ 33–56 and 78–95 regions. On standing for an additional 36 h the solution becomes more orange in color and new resonances appear at δ 44.3 (d, J = 39 Hz), 59.7 (d, J = 57 Hz), and 135.7 (dquin, J = 57, 39 Hz).[14] The minor resonances noted above also increase somewhat in intensity, and the multiplets at δ 61.8 and 129.2 are still prominent. Although data for comparison are limited, we note that the chemical shifts of chelated MeN(P(OMe)$_2$)$_2$ in the five-coordinate complexes **11**, **12**, and **15** fall in the range δ 54–64 while in the four-coordinate complexes **8**, **10** and **14** they occur in the range δ 85–87. In **15** the coordinated end of the monodentate ligand appears at δ 123.0. On this basis we suggest that the major upfield resonances seen in the spectra described above are attributable to chelating MeN(P(OMe)$_2$)$_2$ while the downfield resonances arise from monodentate ligands. Furthermore, except for that responsible for the singlet at δ 118.7, all the major species formed appear to be five-coordinate. The observation of only singlet resonances in the initial solution indicates that no more than one ligand is coordinated to each iridium leading to the suggestion that the δ 51.8 resonance be attributed to [Ir(MeN(P(OMe)$_2$)$_2$(COD)(OClO$_3$)] while the other may be due to a species having the basic skeleton {Ir$_2$(COD)$_2$(μ-MeN(P(OMe)$_2$)$_2$)} with the fourth coordination site on each metal occupied by perchlorate, solvent acetone, or a combination of these. The multiplets that are prominent after 4 h can be approximately reproduced by calculations based on an AA′A″A‴XX′ spin system with coupling constants similar to those determined for **11**, **12**, and **15**. Thus a plausible formulation for the major species at this point is [Ir$_2$(MeN(P(OMe)$_2$)$_2$)$_4$(μ-MeN(P(OMe)$_2$)$_2$]$^{2+}$ with a structure analogous to **3**. In support of this we note that J_{AX} (the coupling between the bridging and chelating ligands) appears comparable to that found in **3** and to J_{12} in **15** although it is not clear why second-order effects are seen here and not in the spectrum of **3**. The formulation of the new species appearing after 36 h is less certain. From the coupling pattern it clearly appears to contain two chelating ligands and a monodentate ligand whose two phosphorus atoms are in quite different environments. A possible formulation is one analogous to **15** but with the free phosphorus oxidized to a phosphoryl moiety. The chemical shift of the resonance assigned to this phosphorus atom is within the range associated with phosphoryl compounds[32] although it is a lower field than the closest analogues. On the other hand none of those involve coordination to a metal and that could very well cause a

---

[31] Brown, M. P.; Fisher, J. R.; Hill, R. H.; Puddephatt, R. J.; Seddon, K. R. *Inorg. Chem.* **1981**, *20*, 3516.

[32] Tebby, J. C. In *Phosphorus-31 NMR Spectroscopy in Stereochemical Analysis*; Verkade, J. G., Quin, L. D., Eds.; VCH Publishers: Deerfield Beach, FL, 1987; Chapter 1.

Table III. Selected Bond Distances (Å) for $[Ir(CO)(MeN(P(OMe)_2)_2)(PPh_3)_2]ClO_4$[a]

atom 1	atom 2	dist	atom 1	atom 2	dist
Ir	P1	2.407 (1)	P3	O31	1.587 (4)
Ir	P2	2.363 (1)	P3	O32	1.583 (4)
Ir	P3	2.277 (2)	P4	N	1.661 (5)
Ir	P4	2.280 (2)	P4	O41	1.573 (4)
Ir	C1	1.901 (6)	P4	O42	1.585 (5)
P1	C111	1.838 (3)	C1	O1	1.134 (7)
P1	C121	1.834 (4)	N	C2	1.494 (8)
P1	C131	1.843 (8)	O31	C31	1.466 (8)
P2	C211	1.82 (1)	O32	C32	1.479 (8)
P2	C221	1.84 (1)	O41	C41	1.451 (8)
P2	C231	1.83 (1)	O42	C42	1.427 (8)
P3	N	1.678 (5)			

[a] Numbers in parentheses are estimated standard deviations in the least significant digits.

downfield shift since the iridium bears a formal positive charge.

If 1 equiv of $MeN(P(OMe)_2)_2$ is slowly added to $[Ir(COD)(acetone)_x]ClO_4$ over a period of 0.5 h, only slight traces of the green color noted earlier are seen and the solution color gradually changes from yellow to reddish brown. The ^{31}P NMR spectrum of the solution after 24 h consists mainly of ill-defined peaks over the range δ 25–110, but a reasonably intense multiplet is seen that can be satisfactorily simulated as an AA′BB′ spin system with δ(A) 89.2, δ(B) 95.2, $J_{AA'} = J_{BB'} = 32.2$, $J_{AB} = 176.6$, and $J_{AB'} = 0.6$ Hz. The derived chemical shifts are close to those exhibited by chelating $MeN(P(OMe)_2)_2$ in the four-coordinate complexes **8**, **10**, and **14**, but there does not appear to be any reasonable formulation of a four-coordinate mono- or dinuclear complex with chelating ligands that is consistent with the observed spin system and coupling constants. It is clear however that the species formed on slow addition of $MeN(P(OMe)_2)_2$ are quite different from those formed when the ligand is added rapidly. Slow addition of a second equivalent of the ligand to the above solution cause the color to become more orange, and its ^{31}P NMR spectrum after 24 h is exceedingly complex. Several new species appear to have formed, but the only one which could be identified was **15**. Again a significant difference from the results of rapid addition of the second equivalent of the ligand are seen since the **15** was formed only initially and subsequently reacted further whereas here it is still present in significant quantity after 24 h.

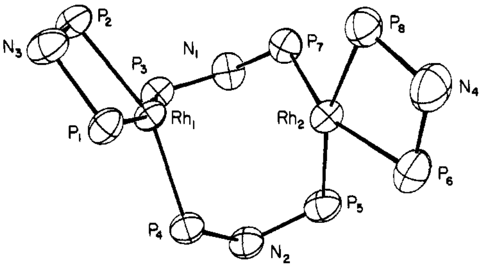

Figure 2. A perspective view of the inner coordination sphere of the $[Rh_2(MeN(P(OMe)_2)_2)_2(\mu\text{-}MeN(P(OMe)_2)_2)_2]^{2+}$ cation (**9**). Thermal ellipsoids are drawn at the 50% probability level.

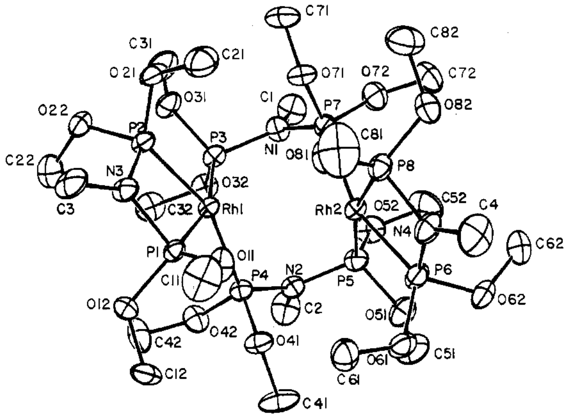

Figure 3. A perspective view of the $[Rh_2(MeN(P(OMe)_2)_2)_2(\mu\text{-}MeN(P(OMe)_2)_2)_2]^{2+}$ cation (**9**). Thermal ellipsoids are drawn at the 30% probability level, and hydrogen atoms are omitted for clarity.

Crystal Structures. The structure of **12** consists of discrete cations and partially disordered anions with no unusually short intermolecular contacts. A perspective view of the cation is shown in Figure 1 while pertinent bond distances and angles are given in Tables III and IV. The coordination about iridium can best be described as a distorted trigonal bipyramid with the axial sites occupied by one triphenylphosphine (P_2) and by one end (P_4) of the $MeN(P(OMe)_2)_2$ ligand. The primary distortion is a bending of P_4 away from the ideal axial position toward P_3 due to the short bite of the bidentate ligand. Others are the bending of the equatorial ligands, particularly P_1, away from P_2[33] and the angular displacement of the car-

Table IV. Selected Interbond Angles (deg) for $[Ir(CO)(MeN(P(OMe)_2)_2)(PPh_3)_2]ClO_4$[a]

atom 1	atom 2	atom 3	angle	atom 1	atom 2	atom 3	angle
P1	Ir	P2	100.97 (5)	Ir	P3	O31	126.3 (2)
P1	Ir	P3	119.75 (6)	Ir	P3	O32	120.9 (2)
P1	Ir	P4	94.45 (6)	N	P3	O31	104.8 (2)
P1	Ir	C1	108.3 (2)	N	P3	O32	109.9 (3)
P2	Ir	P3	94.30 (5)	O31	P3	O32	98.2 (2)
P2	Ir	P4	161.23 (6)	Ir	P4	N	95.7 (2)
P2	Ir	C1	91.1 (2)	Ir	P4	O41	121.9 (2)
P3	Ir	P4	68.54 (6)	Ir	P4	O42	122.5 (2)
P3	Ir	C1	129.4 (2)	N	P4	O41	107.3 (3)
P4	Ir	C1	94.1 (2)	N	P4	O42	109.1 (3)
C111	P1	C121	100.3 (1)	O41	P4	O42	99.4 (2)
C111	P1	C131	102.3 (2)	Ir	C1	O1	175.5 (5)
C121	P1	C131	102.5 (3)	P3	N	P4	100.4 (3)
Ir	P2	C211	117.3 (3)	P3	N	C2	131.1 (5)
Ir	P2	C221	116.1 (3)	P4	N	C2	128.4 (5)
Ir	P2	C231	112.5 (3)	P3	O31	C31	119.0 (4)
C211	P2	C221	103.8 (5)	P3	O32	O32	125.3 (5)
C211	P2	C231	101.7 (4)	P4	O41	C41	127.8 (4)
C221	P2	C231	103.5 (6)	P4	O42	C42	124.9 (5)
Ir	P3	N	95.3 (2)				

[a] Numbers in parentheses are estimated standard deviations in the least significant digits.

Table V. Positional Parameters for $[Rh_2(MeN(P(OMe)_2)_2)_4](F_3CSO_3)_2$

atom	*x*	*y*	*z*	*B*, Å^2	atom	*x*	*y*	*z*	*B*, Å^2
Rh1	0.68781 (2)	0.04195 (2)	0.51661 (4)	2.58 (1)	C42	0.5430 (4)	0.0118 (6)	0.3461 (9)	6.7 (3)
Rh$_2$	0.80545 (3)	−0.03072 (3)	0.43453 (5)	3.06 (1)	C51	0.7554 (6)	−0.0963 (6)	0.0718 (8)	7.1 (3)
P1	0.65418 (9)	−0.03991 (9)	0.6304 (2)	2.84 (3)	C52	0.8501 (5)	0.0404 (7)	0.156 (1)	8.2 (3)
P2	0.6813 (1)	0.08883 (9)	0.6863 (2)	3.26 (4)	C61	0.7346 (4)	−0.2151 (5)	0.4928 (9)	5.5 (2)
P3	0.70732 (9)	0.1441 (1)	0.4352 (2)	3.27 (4)	C62	0.9147 (5)	−0.1421 (6)	0.313 (1)	8.0 (3)
P4	0.65851 (9)	−0.0109 (1)	0.3527 (2)	3.09 (4)	C71	0.8535 (5)	0.1762 (5)	0.620 (1)	7.0 (3)
P5	0.7664 (1)	−0.0172 (1)	0.2569 (2)	3.72 (4)	C72	0.9356 (5)	0.0833 (6)	0.425 (1)	7.3 (3)
P6	0.8233 (1)	−0.1481 (1)	0.4246 (2)	4.06 (5)	C81	0.8471 (6)	−0.1176 (8)	0.7987 (9)	9.5 (3)
P7	0.8230 (1)	0.08616 (9)	0.4560 (2)	3.50 (4)	C82	0.9442 (5)	0.0045 (6)	0.713 (1)	7.3 (3)
P8	0.8574 (1)	−0.0705 (1)	0.5949 (2)	3.84 (4)	S1	0.4510 (1)	0.3249 (1)	0.5657 (2)	4.95 (5)
N1	0.7748 (3)	0.1486 (3)	0.3977 (6)	3.8 (1)	O1	0.4676 (4)	0.3675 (5)	0.6633 (7)	9.9 (2)
N2	0.6939 (3)	0.0027 (4)	0.2410 (5)	3.5 (1)	O2	0.3956 (3)	0.3390 (6)	0.5123 (7)	10.1 (3)
N3	0.6532 (3)	0.0159 (3)	0.7373 (5)	3.6 (1)	O3	0.4654 (5)	0.2558 (4)	0.5859 (9)	10.6 (3)
N4	0.8631 (3)	−0.1525 (3)	0.5486 (6)	4.7 (2)	C5	0.5014 (6)	0.3596 (9)	0.485 (1)	10.1 (4)
C1	0.7916 (5)	0.2033 (5)	0.3192 (7)	5.6 (2)	F1	0.5578 (3)	0.3465 (6)	0.5174 (7)	12.4 (3)
C2	0.6640 (5)	0.0273 (6)	0.1316 (6)	6.3 (3)	F2	0.4955 (4)	0.3157 (8)	0.3904 (8)	15.8 (4)
C3	0.6264 (4)	0.0101 (5)	0.8383 (7)	5.9 (2)	F3	0.4935 (5)	0.4188 (5)	0.4447 (9)	16.5 (3)
C4	0.8988 (5)	−0.2114 (6)	0.598 (1)	7.4 (3)	S2A	0.052	0.675	0.556	6.0*
O11	0.6934 (2)	−0.1067 (3)	0.6686 (4)	4.2 (1)	O4A	0.110	0.671	0.540	9.7*
O12	0.5871 (2)	−0.0674 (3)	0.6173 (5)	4.0 (1)	O5A	0.026	0.740	0.513	9.7*
O21	0.7313 (3)	0.1176 (3)	0.7762 (5)	4.2 (1)	O6A	0.042	0.672	0.671	9.7*
O22	0.6370 (2)	0.1498 (3)	0.7076 (4)	4.3 (1)	C6A	0.011	0.605	0.479	8.3*
O31	0.6997 (3)	0.2079 (2)	0.5195 (5)	4.5 (1)	F4A	0.019	0.601	0.380	12.9*
O32	0.6696 (3)	0.1681 (3)	0.3200 (4)	4.4 (1)	F5A	−0.044	0.599	0.510	12.9*
O41	0.6522 (3)	−0.0929 (3)	0.3659 (4)	4.2 (1)	F6A	0.049	0.544	0.536	12.9*
O42	0.5951 (3)	0.0134 (3)	0.2928 (5)	4.6 (1)	S2B	0.037	0.676	0.433	6.0*
O51	0.7753 (3)	−0.0880 (3)	0.1895 (5)	5.4 (1)	O4B	0.013	0.741	0.435	9.7*
O52	0.7887 (3)	0.0425 (3)	0.1810 (5)	5.3 (1)	O5B	0.101	0.681	0.459	9.7*
O61	0.7782 (3)	−0.2126 (2)	0.4147 (5)	5.1 (1)	O6B	0.017	0.653	0.336	9.7*
O62	0.8633 (3)	−0.1811 (3)	0.3401 (5)	5.2 (1)	C6B	0.009	0.625	0.537	8.3*
O71	0.8381 (3)	0.1062 (3)	0.5821 (4)	4.4 (1)	F4B	0.018	0.637	0.625	12.9*
O72	0.8782 (2)	0.1139 (4)	0.3984 (5)	5.4 (1)	F5B	−0.052	0.632	0.520	12.9*
O81	0.8280 (3)	−0.0710 (3)	0.7066 (4)	5.1 (1)	F6B	0.031	0.563	0.508	12.9*
O82	0.9259 (3)	−0.0525 (3)	0.6339 (6)	5.5 (2)	S2C	0.042	0.627	0.551	6.0*
C11	0.6843 (6)	−0.1509 (5)	0.7606 (8)	7.4 (3)	O4C	0.095	0.593	0.562	9.7*
C12	0.5698 (4)	−0.1341 (5)	0.5645 (9)	5.7 (2)	O5C	0.043	0.679	0.631	9.7*
C21	0.7810 (5)	0.0747 (6)	0.8157 (9)	6.6 (3)	O6C	−0.003	0.580	0.564	9.7*
C22	0.5786 (5)	0.1510 (6)	0.637 (1)	6.9 (3)	C6C	0.028	0.668	0.410	8.3*
C31	0.7099 (5)	0.2799 (4)	0.496 (1)	6.8 (3)	F4C	−0.023	0.703	0.392	12.9*
C32	0.6067 (5)	0.1868 (4)	0.3183 (9)	5.7 (2)	F5C	0.068	0.688	0.349	12.9*
C41	0.6314 (6)	−0.1391 (5)	0.2726 (7)	6.5 (3)	F6C	0.029	0.605	0.366	12.9*

[a] Parameters with an asterisk were refined isotropically. Anisotropically refined atoms are given in the form of the isotropic equivalent displacement parameter defined as $(^4/_3)[a^2B(1,1) + b^2B(2,2) + c^2B(3,3) + ab(\cos\gamma)B(1,2) + ac(\cos\beta)B(1,3) + bc(\cos\alpha)B(2,3)]$.

Table VI. Selected Bond Distances (Å) for $[Rh_2(MeN(P(OMe)_2)_2)_4](F_3CSO_3)_2$[a]

atom 1	atom 2	distance	atom 1	atom 2	distance
Rh1	P1	2.285 (1)	P1	N3	1.690 (4)
Rh1	P2	2.282 (1)	P2	N3	1.682 (4)
Rh1	P3	2.258 (1)	P3	N1	1.653 (4)
Rh1	P4	2.270 (1)	P4	N2	1.689 (4)
Rh2	P5	2.258 (2)	P5	N2	1.674 (5)
Rh2	P6	2.282 (1)	P6	N4	1.668 (5)
Rh2	P7	2.275 (1)	P7	N1	1.711 (4)
Rh2	P8	2.290 (2)	P8	N4	1.674 (5)

[a] Numbers in parentheses are estimated standard deviations in the least significant digits.

bonyl ligand to place it closer to P_1 than to P_3. These appear to be primarily the result of minimizing nonbonded contacts. Thus the $C_1\cdots H_{212}$[34] distance is 2.72 Å and would be less if the carbonyl group were situated more symmetrically between P_1 and P_3. Similar distortions are found in $[Ir(L)(DPPE)_2]X$ (L = CNMe, X = ClO_4;[35] L = CO, X = Cl)[36] and are attributed to interactions with ortho hydrogen atoms on adjacent ligand phenyl groups. The $MeN(P(OMe)_2)_2$ ligand appears rather congested with a number of the contacts between methoxy groups and between these and the nitrogen atom being somewhat less than the sum of van der Waals radii.[37] The most severe intramolecular contact is $O_{32}\cdots H_{226}$ (2.48 Å), and because the methoxy groups are congested as noted above, this probably contributes to the displacement of P_3 from the equatorial plane. The iridium–phosphorus distance to the axial triphenylphosphine ligand ($Ir-P_2$) and the axial–equatorial angle between the two triphenylphosphine ligands (P_2-Ir-P_1) compare well with corresponding values in $[Ir(SiMe_2CH_2CH_2PPh_2)(CO)_2(PPh_3)]$ (2.371 (5) Å; 101.7 (2)°)[38] and $[IrH(CO)_2(PPh_3)_2]$ (2.375 (2)°; 101.38 (7)°).[39] The equatorial iridium phosphine distance ($Ir-P_1$) is significantly longer than $Ir-P_2$ and most other corresponding distances in trigonal-bipyramidal iridium(I) complexes. There appears no obvious explanation for this, but we note that comparable distances were found in $[IrBr(CO)(C_2-$

---

(33) The best plane through the iridium and the equatorial atoms P_1, P_3, and C_1 has the equation $13.1967X - 4.4827Y - 12.6169Z - 2.1365 = 0$ (in crystal coordinates), but this group is not strictly planar as evidenced by the distances of these atoms from the best plane: Ir, 0.0015 (3); P_1, −0.022 (2); P_3, −0.031 (2); C_1, −0.463 (7) Å (negative displacements are in the direction of P_4).

(34) H_{212} is an ortho hydrogen on the phenyl ring built on C_{211}.

(35) Goldberg, S. Z.; Eisenberg, R. *Inorg. Chem.* **1976**, *15*, 58.

(36) Jarvis, J. A. J.; Mais, R. H. B.; Owston, P. G.; Taylor, K. A. *Chem. Commun.* **1966**, 906.

(37) These are $N-O_{31} = 2.591$ (6), $N-O_{32} = 2.670$ (7), $N-O_{41} = 2.605$ (6), $N-O_{42} = 2.644$ (7), $O_{31}-C_{32} = 2.881$ (9), $O_{42}-C_{41} = 2.76$, $C_1-H_{212} = 2.72$, $C_1-H_{122} = 2.746$ (6), and $O_{32}-H_{226} = 2.48$ Å where H_{212}, H_{122}, and H_{226} are ortho hydrogens on the phenyl rings built on C_{211}, C_{121}, and C_{211} respectively.

(38) Auburn, M. J.; Grundy, S. L.; Stobart, S. R.; Zaworotko, M. J. *J. Am. Chem. Soc.* **1985**, *107*, 266.

(39) Payne, N. C.; Ibers, J. A. *Inorg. Chem.* **1969**, *8*, 2714.

Table VII. Selected Interbond Angles (deg) for $[Rh_2(MeN(P(OMe)_2)_2)_4](F_3CSO_3)_2$[a]

atom 1	atom 2	atom 3	angle	atom 1	atom 2	atom 3	angle
P1	Rh1	P2	69.49 (5)	Rh1	P1	N3	94.5 (1)
P1	Rh1	P3	163.19 (5)	Rh1	P2	N3	94.8 (1)
P1	Rh1	P4	98.71 (5)	Rh1	P3	N1	113.9 (2)
P2	Rh1	P3	95.80 (5)	Rh1	P4	N2	122.0 (2)
P2	Rh1	P4	158.96 (5)	Rh2	P5	N2	113.6 (2)
P3	Rh1	P4	92.63 (5)	Rh2	P6	N4	94.6 (2)
P5	Rh2	P6	96.44 (6)	Rh2	P7	N1	122.7 (2)
P5	Rh2	P7	92.37 (5)	Rh2	P8	N4	94.2 (2)
P5	Rh2	P8	164.10 (6)	P3	N1	P7	114.4 (2)
P6	Rh2	P7	159.82 (6)	P4	N2	P5	115.4 (2)
P6	Rh2	P8	69.14 (6)	P1	N3	P2	101.1 (2)
P7	Rh2	P8	99.34 (6)	P6	N4	P8	101.8 (2)

[a] Numbers in parentheses are estimated standard deviations in the least significant digits.

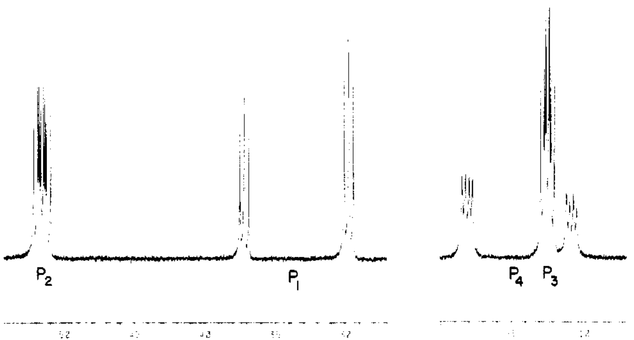

Figure 4. The 81.02-MHz $^{31}P\{^1H\}$ NMR spectrum (30 °C) of $[Ir(DMAD)(MeN(P(OMe)_2)_2)(BDPPF)]^+$ in deuterioacetone. The chemical shift assignment corresponds to that of structure A.

$(CN)_4)(PPh_3)_2]$ (2.397 (3), 2.402 (3) Å).[40] The Ir–P_3 and Ir–P_4 distances are comparable to those found in $[(\eta^3\text{-}C_3H_5)Ir(COD)(P(OMe)_3)_2]$ (2.276 (2) Å)[41] and in $[Ir(CO)(P(OMe)_3)_2(\mu\text{-S-}t\text{-Bu})_2Ir(CO)(C_2(CN)_4)]$ 2.252 (4), 2.301 (4) Å)[42] while bond distances within the $MeN(P(OMe)_2)_2$ ligand are quite similar to those found in $[Co_2(CO)_4(MeN(P(OMe)_2)_2)_2]$.[3] All other metrical parameters are unexceptional except some of those associated with the disordered portion of the perchlorate ion and the phenyl rings are planar within experimental error.

The structure of **9** consists of discrete dimeric cations interspersed with trifluoromethanesulfonate anions, one of which is at least threefold disordered, with no unusually short intermolecular contacts. Figure 2 shows the core of the cation while a view of the complete cation is presented in Figure 3. From both of these it is apparent that the basket-shaped cation possesses approximate C_2 symmetry. This can also be seen from the various Rh–P distances and P–Rh–P angles presented in Tables VI and VII. The $Rh_1\cdots Rh_2$ separation of 3.2727 (5) Å is clearly nonbonding and can be compared with those found previously in *trans*-$[(OC)ClRh(\mu\text{-}L_2)_2Rh(CO)Cl]$ (L_2 = DPM, 3.2386 (5) Å;[43] L_2 = DAM, 3.396 (1) Å).[44] As in those cases, the absence of an attractive metal–metal interaction is further confirmed by the fact that the $Rh_1\cdots Rh_2$ distances is significantly longer than the intraligand phosphorus–phosphorus distances of the bridging ligands ($P_3\cdots P_7$ = 2.829 (2), $P_4\cdots P_5$ = 2.842 (2) Å). The coordination about each metal can be described as severely distorted square planar with one chelating and two cis-disposed bridging $MeN(P(OMe)_2)_2$ ligands. Other examples of this relatively rare cis arrangement of bridging ligands include $[Pt_2Me_4(DPM)_2]$,[45] $[Ni_2(CNMe)_2(\mu\text{-CNMe})(DPM)_2]$,[46] and $[Rh_2(CO)_2(bipy)(\mu\text{-}RN_3R)_2]$ (R = *p*-tolyl).[47]

One distortion of the coordination sphere of each rhodium atom is the result of the short bite of the chelate ligand while a second is the significant departure of each set of four phosphorus atoms from planarity[48] and a displacement of each rhodium atom from these best planes toward the center of the cation.[48] These planes are not parallel as is the case in *trans*-$[(OC)ClRh(\mu\text{-}L_2)_2Rh(CO)Cl]$ (L_2 = DPM,[43] DAM[44]) but are inclined at an angle of 32.92 (4)°. Also, one side of the cation is twisted about the metal–metal axis with respect to the other by 27.51 (8)°. Both these features seem to be primarily the result of minimizing intramolecular contacts. Despite this, the cation remains quite congested with a number of inter- and intraligand contacts being significantly less than the sum of the appropriate van der Waals radii (Table XIX, supplementary material). The most severe are $O_{21}\cdots O_{22}$ (2.282 (6) Å) and $O_{61}\cdots O_{62}$ (2.313 (6) Å). Interestingly, all these close contacts also conform to the approximate C_2 symmetry of the cation.

With the exception of Rh_1–P_3 and Rh_2–P_5 which are significantly shorter than the rest, all of the Rh–P distances are essentially equivalent. There is no obvious reason for this difference but all are comparable to those found previously in $[Rh_2Cl_2(CO)(\mu\text{-}CO)(\mu\text{-}(MeO)_2PH(Et)P(OMe)_2)_2]$ (2.28–2.30 Å),[4] $[Rh_2Cl_2(CO)(\mu\text{-}(PhO)_2PN(Et)P(OPh)_2)_2]$ (2.184–2.258 Å),[5c] and $[Rh_2(CO)_3(\mu\text{-}(PhO)_2PN(Et)P(OPh)_2)_2]$ (2.247 (5)–2.267 (5) Å).[5a] Other intraligand distances compare well with those found in **12**, $[Co_2(CO)_4(\mu\text{-}(MeO)_2PN(Me)P(OMe)_2)_2]$,[3] and $[Rh_2Cl_2(CO)(\mu\text{-}CO)(\mu\text{-}(MeO)_2PN(Et)P(OMe)_2)_2]$.[4]

The trifluoromethanesulfonate ion based on S_1 refined reasonably well, but the derived geometry showed some deviations from the expected geometry. As some of the thermal ellipsoids, particularly those of the fluorine atoms, were quite large, it is likely that some disorder is present that can explain the observed distortions, behavior which has been observed previously.[49]

---

(40) McGinnety, J. A.; Ibers, J. A. *Chem. Commun.* **1968**, 235.

(41) Muetterties, E. L.; Tau, K. D.; Kirner, J. F.; Harris, T. V.; Stark, J.; Thompson, M. R.; Day, V. W. *Organometallics* **1982**, *1*, 1562.

(42) Maisonnat, A.; Bonnet, J.-J.; Poilblanc, R. *Inorg. Chem.* **1980**, *19*, 3168.

(43) Cowie, M.; Dwight, S. K. *Inorg. Chem.* **1980**, *19*, 2500.

(44) Mague, J. T. *Inorg. Chem.* **1969**, *8*, 1975.

(45) Manojlovic-Muir, L.; Muir, K. W.; Frew, A. A.; Ling, S. S. M.; Thomson, M. A.; Puddephatt, R. J. *Organometallics* **1984**, *3*, 1637.

(46) DeLaet, D. L.; Fanwick, P. E.; Kubiak, C. P. *Organometallics* **1986**, *5*, 1807.

(47) Connelly, N. G.; Garcia, G. *J. Chem. Soc., Chem. Commun.* **1987**, 246.

(48) The best planes through the atoms P_1–P_4 and P_5–P_8 have the equations $-21.3102X + 5.9573Y - 0.2649Z + 14.2596 = 0$ and $21.2328X + 0.6970Y - 5.6594Z - 14.8810 = 0$ (in crystal coordinates). The distances (Å) of these atoms from their respective planes are as follows: P_1, −0.086 (2); P_2, 0.088 (2); P_3, −0.070 (2); P_4, 0.068 (2); and P_5, −0.075 (2); P_6, 0.094 (2); P_7, 0.073 (2); P_8, −0.092 (2). Rh_1 is −0.2848 (6) Å from the first plane, and Rh_2 is −0.2597 (6) Å from the second (negative displacements are toward the center of the cation).

Conclusions

The ligands $RN(P(OMe)_2)_2$ (R = Me, Ph) do not appear to be as generally useful as DPM for forming binuclear, A-frame type complexes. With the exception of **9** the only binuclear complexes formed contained a single bridging ligand. Among the mononuclear complexes prepared a number appear to adopt highly fluxional, trigonal-bipyramidal structures as a consequence of the short bite of the chelating ligand. One useful result of this work has been the direct determination of values, some of which are quite large, for $^2J_{P-P}$ between trans-disposed phosphorus atoms in four- and five-coordinate rhodium and iridium complexes.

Acknowledgment. We thank the Tulane University Chemistry Department and the Pennzoil Corp. for financial support, Dr. Marie K. Johnson for collecting the X-ray data on the rhodium complex, and Prof. D. M. Roundhill for helpful discussions.

Registry No. **1**, 112968-94-2; **2**, 112947-29-2; **3**, 112947-31-6; **4**, 112947-33-8; **5**, 112947-35-0; **6**, 112947-37-2; **7**, 112947-39-4; **8**, 112947-41-8; **9**, 112947-43-0; **10**, 112947-45-2; **11**, 112947-47-4; **12**, 112947-49-6; **13**, 112947-51-0; **14**, 112947-53-2; **15**, 112947-55-4; BDPPF, 12150-46-8; $[RhCl(COD)]_2$, 12092-47-6; $[Rh(COD)(DPPE)]ClO_4$, 32799-70-5; $[Rh_2(COD)_2(\mu\text{-}Ph_2PC_4H_2OPPh_2)_2](ClO_4)_2$, 112947-57-6; $[Ir_2(COD)_2(\mu\text{-}Ph_2PC_4H_2OPPh_2)_2]ClO_4)_2$, 112947-59-8; $[Ir(COD)(PPh_3)_2]ClO_4$, 52657-94-0; $[Ir(CO)_3(PPh_3)_2]ClO_4$, 15738-08-6; $[IrCl(COD)]_2$, 12112-67-3; $PhN(P(OMe)_2)_2$, 112947-58-7; $MeN(P(OMe)_2)_2$, 34244-05-8; $P(OMe)_3$, 121-45-9.

Supplementary Material Available: Tables of anisotropic thermal parameters, rms amplitudes of anisotropic displacement, intraligand bond distances and interbond angles, torsion angles, and calculated hydrogen atom positions for **9** and **12** (31 pages); listings of F_o vs. F_c for **9** and **12** (139 pages). Ordering information is given on any current masthead page.

---

(49) Ardon, M.; Bino, A.; Cotton, F. A.; Dori, Z.; Kaftory, M.; Reisner, G. *Inorg. Chem.* **1982**, *21*, 1912.

Oxidative Addition of Nitroalkanes to Dinuclear Gold(I) Ylide Complexes. The Characterization by X-ray Crystallography of $Au_2(ylide)_2(NO_2)_2$, a Nitro Complex of Gold(II)

Barbara Trzcinska-Bancroft, Md. Nazrul I. Khan, and John P. Fackler, Jr.*

Department of Chemistry, Laboratory for Molecular Structure and Bonding, Texas A&M University,
College Station, Texas 77843

Received November 25, 1987

The Au^I ylide complex $[Au((CH_2)_2PPh_2)]_2$ (1) reacts oxidatively with nitroalkanes to form a Au^{II} product, $[Au((CH_2)_2PPh_2)NO_2]_2$ (**2-NO$_2$**). This complex was characterized by IR, NMR, and X-ray crystallography. The identity of the product was confirmed by the quantitative formation of **2-NO$_2$** from 1 and N_2O_4 "brown gas". The product crystallizes in a monoclinic system *C*2/*c*: a = 12.159 (2) Å, *b* = 14.638 (2) Å, *c* = 16.536 (2) Å, *β* = 103.757 (11)°, and *Z* = 4 with *R* = 0.036 and R_w = 0.033.

Introduction

The two-center oxidative addition chemistry of $[Au((CH_2)_2PPh_2)]_2$ (1) is well-established.[1] Reactions with halogens,[2] benzoyl peroxide,[3] and thiuram disulfide[3b] gives symmetrical gold(II)–gold(II) dimers $[Au((CH_2)_2PPh_2)X]_2$ (**2-X**, X = Cl, Br, I, $OC(O)C_6H_5$, SeC_6H_5, etc.). Methyl halides also react[4] with 1 to form metal–metal bonded adducts $[Au((CH_2)_2PPh_2)]_2CH_3X$ (X = I, Br). These studies have revealed that 1 reacts with many solvents.

Our initial studies of reactions of CH_3NO_2 with gold ylide complexes focussed on reactions with the Au^{II} complex $[Au((CH_2)_2PPh_2)OC(O)C_6H_5]_2$ (**2-OBz**). As reported,[3] a nitromethane solution of **2-OBz** at 0 °C produces the A-frame complex wherein $CHNO_2$ bridges two Au(III) centers. At room temperature a somewhat different chemistry takes place. When left standing in a THF/CH_3NO_2 (12:1) solvent mixture, **2-OBz** gives the title compound **2-NO$_2$**.

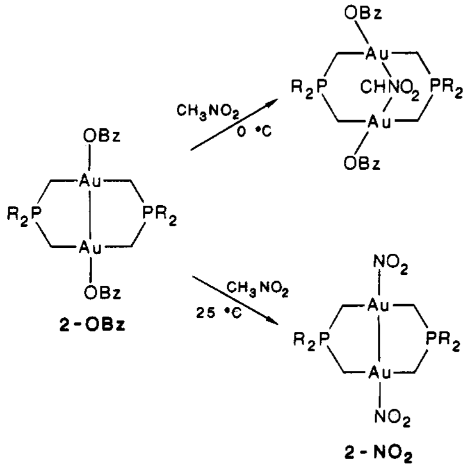

---

(1) (a) Basil, J. D. Ph.D. Thesis, Case Western Reserve University, Cleveland, OH, 1982. (b) Kaska, W. C. *Coord. chem. Rev.* **1983**, *48*, 1–58. (c) Schmidbaur, H. *Acc. Chem. Res.* **1975**, *8*, 62–70.

(2) (a) Fackler, J. P., Jr.; Basil, J. D. *Inorganic Chemistry, Toward the 21st Century*; Chisholm, M. U., Ed.; ASC Symposium Series 211; American Chemical Society: Washington, DC 1983. (b) Schmidbaur, H.; Franke, R. *Inorg. Chim. Acta* **1975**, *13*, 85–89.

(3) (a) Knachel, H. C.; Dudis, D. S.; Fackler, J. P., Jr. *Organometallics* **1984**, *3*, 1312–1313. (b) Heinrich, D.; Porter, L. C.; Fackler, J. P. Jr., in preparation.

(4) (a) Fackler, J. P., Jr.; Basil, J. D. *Organometallics* **1982**, *1*, 871–873. (b) Fackler, J. P., Jr.; Murray, H. H.; Basil, J. D. *Organometallics* **1984**, *3*, 821–823.

0276-7333/88/2307-0993$01.50/0 © 1988 American Chemical Society